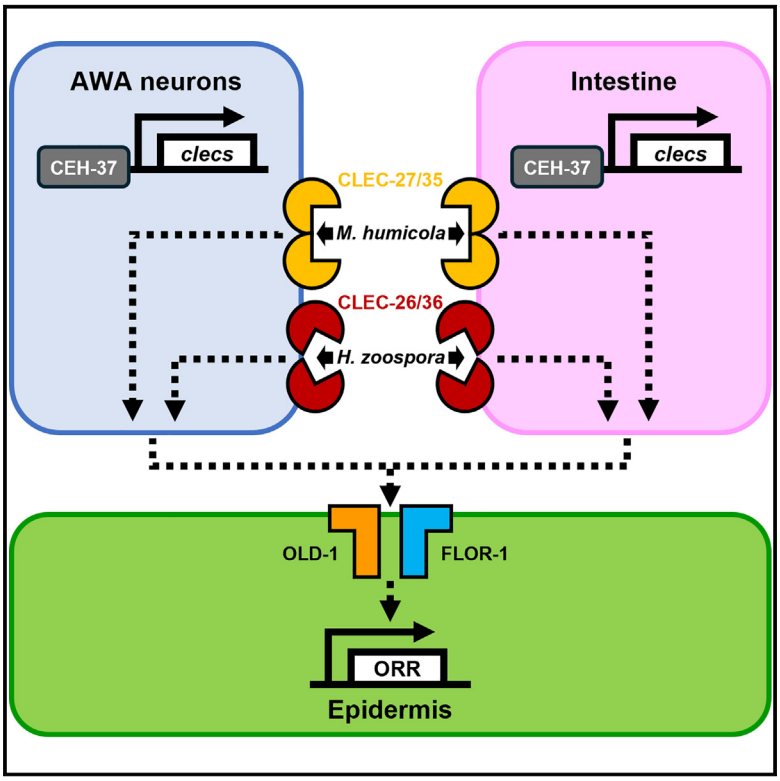
Cell Reports

Article

Paired C-type lectin receptors mediate specific recognition of divergent oomycete pathogens in *C. elegans*

Graphical abstract



Authors

Kenneth Liu, Manish Grover, Franziska Trusch, Christina Vagena-Pantoula, Domenica Ippolito, Michalis Barkoulas

Correspondence

m.barkoulas@imperial.ac.uk

In brief

Liu et al. show that *C. elegans* specifically recognizes divergent oomycete pathogens through paired transmembrane C-type lectin receptors. These act mainly in AWA neurons and the intestine to induce in the epidermis a protective immune response characterized by the induction of *chitinase-like* (*chil*) genes.

Highlights

- A CLEC-27/CLEC-35 pair is required for recognition of the oomycete *Myzocytiopsis humicola*
- A CLEC-26/CLEC-36 pair is required for recognition of the oomycete *Haptoglossa zoospora*
- Both CLEC pairs are co-regulated by the homeodomain transcription factor CEH-37/OTX2
- Both CLEC pairs function redundantly in AWA neurons and the intestine for host defense

Liu et al., 2024, Cell Reports *43*, 114906
November 26, 2024 © 2024 The Author(s). Published by Elsevier Inc.
https://doi.org/10.1016/j.celrep.2024.114906

CellPress

Cell Reports

CellPress
OPEN ACCESS

Article

Paired C-type lectin receptors mediate specific recognition of divergent oomycete pathogens in *C. elegans*

Kenneth Liu,[1,2] Manish Grover,[1,2] Franziska Trusch,[1] Christina Vagena-Pantoula,[1] Domenica Ippolito,[1] and Michalis Barkoulas[1,3,*]

[1]Department of Life Sciences, Imperial College, SW7 2AZ London, UK
[2]These authors contributed equally
[3]Lead contact
*Correspondence: m.barkoulas@imperial.ac.uk
https://doi.org/10.1016/j.celrep.2024.114906

SUMMARY

Innate immune responses can be triggered upon detection of pathogen- or damage-associated molecular patterns by host receptors that are often present on the surface of immune cells. While invertebrates like *Caenorhabditis elegans* lack professional immune cells, they still mount pathogen-specific responses. However, the identity of host receptors in the nematode remains poorly understood. Here, we show that C-type lectin receptors mediate species-specific recognition of divergent oomycetes in *C. elegans.* A CLEC-27/CLEC-35 pair is essential for recognition of the oomycete *Myzocytiopsis humicola*, while a CLEC-26/CLEC-36 pair is required for detection of *Haptoglossa zoospora.* Both *clec* pairs are transcriptionally regulated through a shared promoter by the conserved PRD-like homeodomain transcription factor CEH-37/OTX2 and act in sensory neurons and the anterior intestine to trigger a protective immune response in the epidermis. This system enables redundant tissue sensing of oomycete threats through canonical CLEC receptors and host defense via cross-tissue communication.

INTRODUCTION

In their natural habitats, all organisms face a plethora of microbes; therefore, it is advantageous to distinguish what is potentially harmful from what is not.[1] To detect pathogens, the innate immune system is equipped with pathogen recognition receptors that sense pathogen-associated molecular patterns (PAMPs) and enable animals to either avoid pathogens or combat them with anticipatory immune responses.[2] Such receptors, including the Toll-like receptors (TLRs), the nucleotide-binding and oligomerization domain-like receptors, and C-type lectin receptors, are found mainly in professional immune cells in mammals.[2] However, many invertebrates such as the nematode *Caenorhabditis elegans* do not have professional immune cells and instead rely on non-professional cells for defense, such as epithelial cells and neurons, which act together to mount protective immune responses.[3–5] While there is clear evidence that *C. elegans* can sense microbial products[6–9] and mount defense responses in a pathogen-specific way,[10–14] the mechanisms through which this specificity is achieved remain elusive.[15] This is largely because canonical pattern recognition receptors are either absent or have not been directly linked to immunity in *C. elegans*.[16,17] For example, a single TLR gene named *tol-1* has been shown to modulate the behavioral response to pathogenic bacteria; however, this role is not directly linked to pathogen recognition, differing from how TLRs function in other invertebrates and vertebrates.[18,19] Our understanding of pathogen recognition receptors in *C. elegans* is therefore still in its infancy, with only a few well-established examples reported so far, such as the G protein-coupled receptor DCAR-1 that senses a cuticle-damage-induced metabolite produced upon infection with the fungus *Drechmeria coniospora*,[20] the RIG-I homolog DRH-1 that recognizes Orsay virus replication products,[21] and the nuclear hormone receptor NHR-86 that directly binds a metabolite from *Pseudomonas aeruginosa* to activate a protective transcriptional program.[22]

One example of a gene family in *C. elegans* that has the potential to encode pattern recognition receptors is the C-type lectin family.[23] In vertebrates, CLEC proteins play fundamental roles in immunity acting either as secreted antimicrobial effectors or as transmembrane pathogen recognition receptors binding mostly to sugar moieties from a wide range of pathogens.[24,25] However, much less is known about CLEC proteins in invertebrates, where expansion of *clec* gene families can be found.[26–29] In *C. elegans*, the *clec* gene family contains more than 280 members, making it one of the largest gene families in the nematode.[30] While several *clec* genes are differentially expressed upon exposure to different pathogens,[23,30–36] their exact roles in immunity are still poorly understood, and this is particularly pertinent to transmembrane CLEC proteins as most studies have focused on secreted CLEC proteins. Members of the *clec* gene family have been shown to modulate host defense against

This is an open access article under the CC BY license (http://creativecommons.org/licenses/by/4.0/).

bacterial pathogens.[11,32,36–39] In some cases, CLEC proteins display antimicrobial activity and can directly bind to bacterial pathogens.[11,36–38,40] Alternatively, CLEC proteins are also able to modulate immunity in other ways, such as through regulating proteostasis, as shown for CLEC-1 that is secreted by body muscle cells to prevent aggregation of LYS-7 required for fighting against *Bacillus thuringienesis*,[41] or through changes in animal behavior.[33,42] Given that most C-type lectin domains in *C. elegans* are divergent in sequence in comparison to those found in mammalian proteins,[23,30,43] and that CLEC proteins can play roles beyond immunity (for example in the context of development and aging[44–46]), it is still unclear whether they act as pattern recognition receptors in the nematode and whether expansion of the *clec* gene family relates to immune response specificity.

Here, we address this question in the context of natural infection of *C. elegans* by two phylogenetically distinct oomycetes,[47] namely *Myzocytiopsis humicola*[12] and *Haptoglossa zoospora*.[48] Upon oomycete exposure, *C. elegans* activates a specific transcriptional response (ORR, oomycete recognition response) characterized by the epidermal expression of some *chitinase-like* (*chil*) genes that protect *C. elegans* from oomycete infection.[48,49] We demonstrate that paired CLEC proteins act as plausible receptors for oomycete recognition in *C. elegans*, where a CLEC-27 and CLEC-35 pair specifically recognizes *M. humicola*, and a CLEC-26 and CLEC-36 pair specifically recognizes *H. zoospora*. Both *clec* pairs are regulated by the conserved PRD-like homeodomain protein CEH-37/OTX2[50] through a single shared promoter for each pair and predominantly function in the intestine and the AWA sensory neurons, providing a redundant sensing system that leads to epidermal *chil-27* gene activation through cross-tissue communication. These findings highlight that C-type lectin proteins act as pattern recognition receptors in *C. elegans* and that the diversification of the *clec* gene family contributes to immune specificity.

RESULTS AND DISCUSSION

C. elegans lacking either *ceh-37*, *clec-27*, or *clec-35* fail to induce the oomycete recognition response

Through a forward genetic approach aimed at identifying animals that fail to respond to an innocuous *M. humicola* extract that is known to induce the ORR[49] (Figure S1A), we found independent mutants harboring premature stop codons within the *clec-27* and *clec-35* genes that resulted in complete loss of *chil-27p::GFP* induction (Figures 1A, 1B, and S1B). CLEC-27 and CLEC-35 belong to the membrane-associated type of C-type lectin proteins with a double CLEC domain on the extracellular side.[30] The alleles we recovered carry loss-of-function mutations given that *clec-27* or *clec-35* RNAi led to loss of *chil-27p::GFP* induction upon exposure to *M. humicola* extract (Figure S1C). Furthermore, expression of wild-type *clec-27* and *clec-35* in the respective mutants fully rescued the induction of *chil-27p::GFP* (Figures 1C and S1D). In addition to *clec* genes, we also found non-synonymous changes in the PRD-like homeodomain protein CEH-37[51] (Figures 1A and 1B), which has been shown to play roles in sensory neuron specification,[50] telomere function,[52] and intestinal immunity against bacterial pathogens.[53] These mutations also created loss-of-function alleles as *chil-27p::GFP* was not induced upon exposure to *M. humicola* extract when *ceh-37* expression was knocked down by RNAi (Figure S1C) or in animals carrying a previously described *ceh-37(ok642)* deletion allele[54] (Figure S1B). Fosmid-based overexpression of the *ceh-37* genetic locus in *ceh-37(icb36)* mutants fully rescued *chil-27* induction upon pathogen extract exposure (Figures 1C and S1D).

Next, we investigated whether the induction of the ORR was more broadly impaired in the identified mutants. We performed RNA-seq analysis in *clec-27(icb104)*, *clec-35(icb105)*, and *ceh-37(ok642)* animals exposed to *M. humicola* extract in comparison to extract-exposed wild-type animals. We found that most of the 50 reproducibly induced genes from the stringent ORR gene list[55] were not upregulated in the mutants (Figure S1E). Consistent with a defect in mounting the ORR, these mutants were hypersusceptible to infection by *M. humicola* (Figure 1D). While CEH-37 has also been shown to be required for immunity against bacterial pathogens,[53] this did not require CLEC-27 or CLEC-35, as loss-of-function mutants of both did not show any difference in their susceptibility toward *P. aeruginosa* compared to wild-type animals (Figure S2). Therefore *clec-27* and *clec-35* are genes specifically required for the induction of the protective ORR in response to *M. humicola* extract exposure.

clec-27 and *clec-35* are co-expressed in the neurons and the intestine where they are regulated by CEH-37

Interestingly, *clec-27* and *clec-35* are neighboring loci on chromosome V and are transcribed in opposite directions, suggesting that they are likely to be co-expressed via a shared promoter (Figure 1A). To test this possibility, we generated a transcriptional reporter where the *clec-27* coding sequence was replaced with GFP and the *clec-35* sequence with mScarlet. Transgenic animals showed GFP and mScarlet co-localization both in neurons in the head area as well as the anterior intestine (Figure 2A). This neuronal and intestinal *clec-27/35* localization suggested that they may regulate epidermal *chil-27* gene activation in a cross-tissue manner. To address if *clec-27/35* are required in the intestine and/or neurons, we performed tissue-specific rescue experiments in *clec-35(icb105)* mutants. We found that both neuronal (*rab-3p*) and intestinal (*vha-6p*) *clec-35* expression rescued *chil-27p::GFP* induction upon exposure to *M. humicola* extract, whereas epidermal (*dpy-7p*) expression did not (Figures 2B and 2C). The rescue was also observed at the level of survival in the presence of *M. humicola*, wherein both neuronal and intestinal *clec-27/35* expression reversed the hypersusceptibility of *clec-35(icb105)* mutants (Figure 2D). Both intestine-specific and neuron-enhanced *clec-27* and *clec-35* RNAi significantly reduced *chil-27p::GFP* expression (Figure 2E). To further evaluate interaction between CLEC-27 and CLEC-35, different combinations of GFP and myc-tagged CLEC proteins were co-expressed in *N. benthamiana* due to low expression levels in *C. elegans* and insolubility of CLEC proteins in prokaryotic expression systems. Reverse pull-downs upon co-immunoprecipitation (coIP) with GFP and myc beads confirmed interaction between CLEC-27 and CLEC-35 (Figure S3). Furthermore, it is unlikely that CLEC-27 or CLEC-35 homodimers function in *M. humicola* recognition as overexpression of *clec-35* in *clec-27(icb104)* and *clec-27* in *clec-35(icb105)* failed to rescue

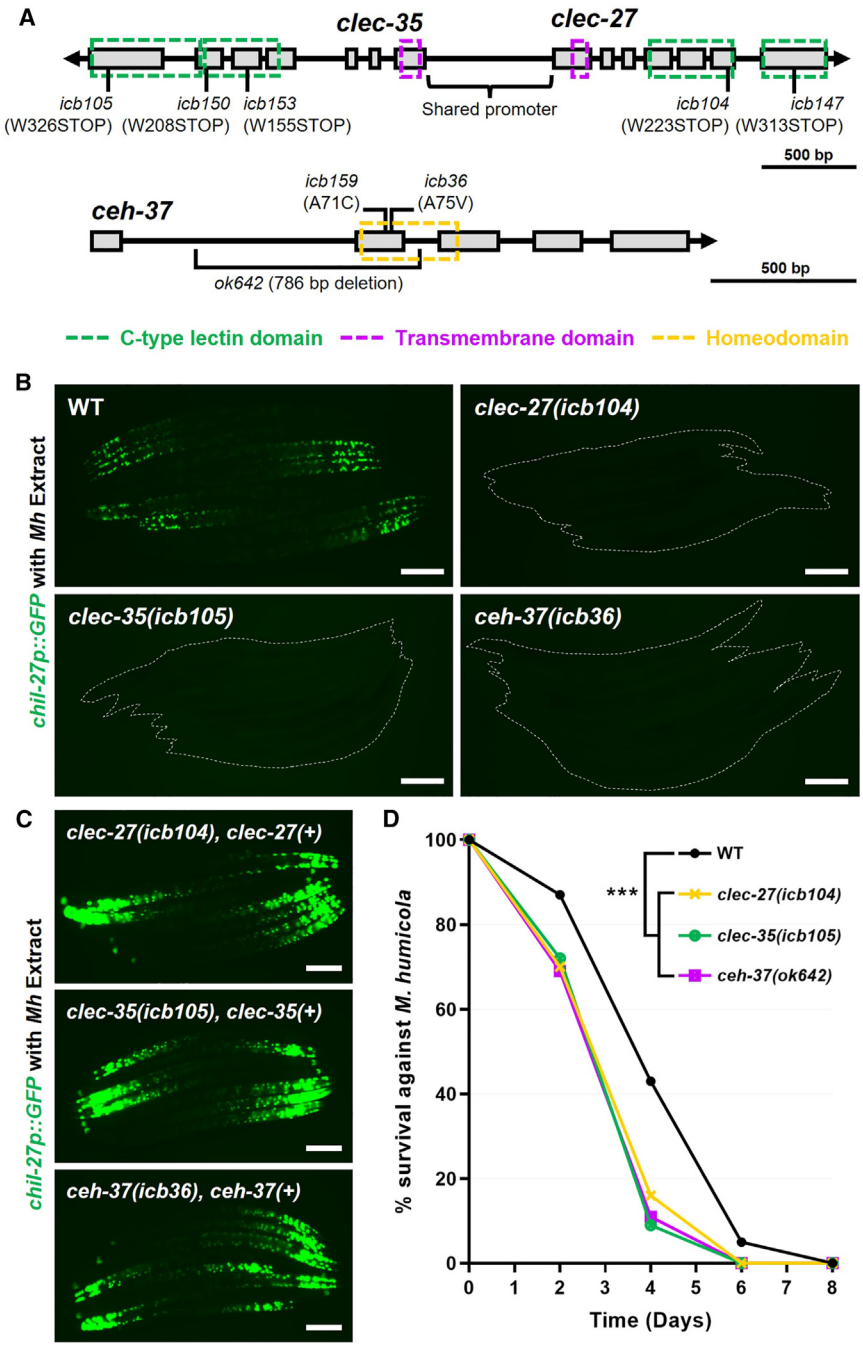


Figure 1. Loss of function of *clec-27*, *clec-35*, or *ceh-37* impairs the *C. elegans* response to *M. humicola* extract

(A) Gene structure of *ceh-37*, *clec-27*, and *clec-35* showing the positions of mutant alleles generated in this study.

(B) L4 stage *clec-27(icb104)*, *clec-35(icb105)*, and *ceh-37(icb36)* mutant animals showing lack of *chil-27p::GFP* induction upon exposure to *M. humicola* (*Mh*) extract.

(C) Rescue of *chil-27p::GFP* induction by providing the wild-type gene locus in the respective mutant backgrounds.

(D) *clec-27(icb104)*, *clec-35(icb105)*, and *ceh-37(ok642)* mutant animals exhibit hypersusceptibility to infection by *M. humicola* (n = 60 per condition, performed in biological triplicates, $^{***}p < 0.001$ based on log rank test). Scale bars in (B) and (C) represent 100 μm.

chil-27p::GFP induction upon exposure to *M. humicola* extract (Figure S1D). These results suggest that CLEC-27 and CLEC-35 are likely to act as heterodimers in both the neurons and the intestine for oomycete recognition.

Similar to *clec-27/35* RNAi, *ceh-37* RNAi in both neuron-enhanced and intestine-specific RNAi strains significantly reduced *chil-27p::GFP* induction (Figure 2E). Notably, we observed in our RNA-seq datasets that in uninduced conditions, several *clec* genes, including *clec-27* and *clec-35*, were downregulated in the *ceh-37(ok642)* mutant background (Table S1).

Furthermore, *ceh-37* is expressed in both head neurons[56] and the intestine[53] (Figure S4A), and in the shared *clec-27/35* promoter, a sequence similar to the consensus sequence required for the DNA binding of the CEH-37 homolog OTX2 in mammals[57] is present (Figure S4B). Therefore, we reasoned that CEH-37 may regulate the expression of *clec* genes in these tissues. We introduced the *clec-27/35* transcriptional reporter into the *ceh-37(ok642)* deletion mutant and found significant reduction of *clec-27p::GFP* expression in the anterior intestine and in the head region (Figure 2F). Furthermore, restoring *clec-27/35* expression in neurons (*rab-3p*) or intestine (*vha-6p*) in *ceh-37(icb36)* mutants was sufficient to rescue *chil-27p::GFP* induction upon exposure to *M. humicola* extract (Figure 2G). Taken together, these results suggest that the loss of *chil-27p::GFP* induction upon oomycete recognition in *ceh-37* mutants is because CEH-37 regulates the expression of *clec-27/35* in both neurons and the intestine.

We have previously shown that ORR activation can also be triggered through perturbations directly in the epidermis, such as proteasome dysfunction,[58] modulation of the PALS-22/25 module,[59,60] or constitutive signaling by the receptor tyrosine kinase OLD-1.[55] We hypothesized that CLEC-27/35 are likely to act prior to the activation of immune response in the epidermis. To test this hypothesis, we performed *clec-27* and *clec-35* RNAi in animals showing constitutive expression of *chil-27p::GFP* due to overexpression of *old-1* (Figure 2H) or, conversely, *pals-22* and *skn-1* RNAi in the *clec-27* and *clec-35* mutant backgrounds recovered from our genetic screen (Figure 2I). In all cases, we observed

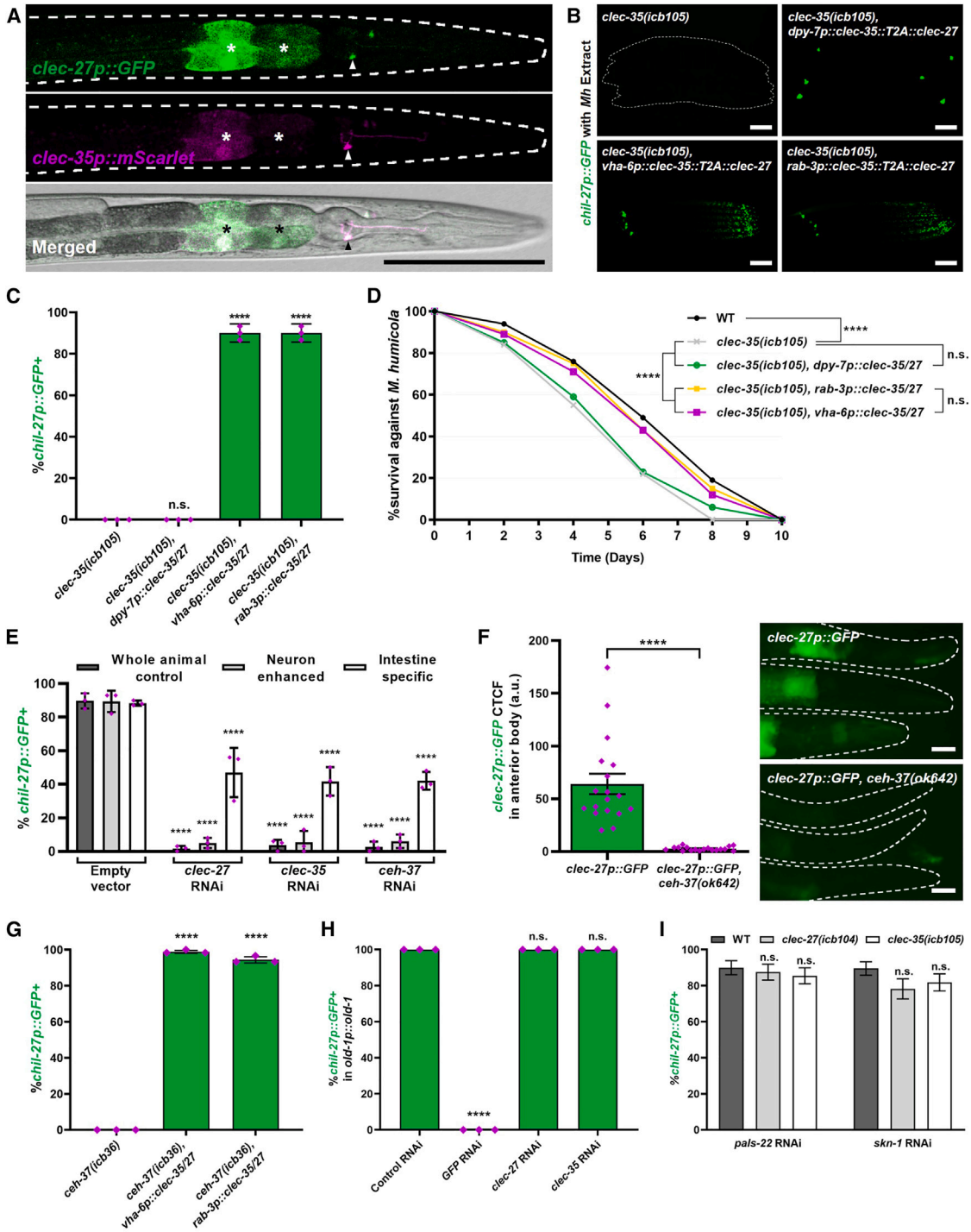


Figure 2. *clec-27* and *clec-35* are co-expressed in neurons and intestine and are regulated by CEH-37

(A) Expression of a transcriptional reporter of *clec-27/35* (*mScarlet::clec-27/35p::GFP*) shows fluorescent protein co-localization in the anterior intestine (marked by asterisks) as well as neurons (arrow).

(B and C) Both neuronal (*rab-3p*) and intestinal (*vha-6p*) expression of *clec-27/35* rescues induction of *chil-27p::GFP* in *clec-35(icb105)* mutants upon exposure to *M. humicola* extract ($n = 60$ animals, performed in biological triplicates, $^{****}p < 0.0001$ based on chi-squared test).

(D) Neuronal and intestinal expression of *clec-27/35* in *clec-35(icb105)* mutants rescues their hypersusceptibility to *M. humicola* infection, whereas epidermal expression does not ($n = 60$ per condition, performed in biological triplicates, $^{****}p < 0.0001$ based on log rank test).

(E) *chil-27p::GFP* induction upon *M. humicola* extract exposure following tissue-specific RNAi of *clec-27*, *clec-35*, and *ceh-37* ($n = 50$ per condition, performed in biological triplicates, $^{****}p < 0.0001$ based on chi-squared test).

(legend continued on next page)

normal *chil-27p::GFP* induction, confirming that the role of *clec-27/35* in the neurons and intestine lies upstream of the epidermal triggers of the ORR.

AWA is the main oomycete-sensing neuron in *C. elegans*

To identify the specific neurons involved in *M. humicola* extract recognition, we focused on AWA, AWB, ASG, and BAG, which are the four neurons that express CEH-37.[56] We attempted to rescue *clec-27(icb104)* mutants by restoring *clec-27* under the neuron-specific promoters *odr-7p* (AWA),[61] *str-1p* (AWB),[62] *gcy-15p* (ASG),[63] and *gcy-33p* (BAG).[64] As controls, we restored *clec-27* expression in *clec-27(icb104)* mutants under the *ceh-37* promoter in case multiple neurons are required, or under the *srg-8p* promoter (ASK),[65] where *ceh-37* is not normally expressed.[56] Here we found that *clec-27/35* rescue in the AWA neurons most strongly recovered *chil-27p::GFP* induction upon exposure to *M. humicola* extract followed by rescue in AWB neurons (Figure 3A). Furthermore, restoring *clec-27/35* expression in *ceh-37(icb36)* mutants in either AWA or AWB neurons was sufficient for animals to strongly recover *chil-27p::GFP* induction upon exposure to *M. humicola* extract (Figure 3B).

To confirm that *clec-27/35* are expressed in these neurons, we co-localized the neuron-specific markers *odr-10p::GFP* (AWA)[66] and *str-1p::GFP* (AWB) with *clec-27/35p::mScarlet*. We found *clec-35* expression in both AWA and AWB neurons (Figure 3C). To test the functional significance of the AWA/AWB neurons, we genetically ablated them by cell-specific expression of a caspase and assessed whether animals can mount *chil-27p::GFP* expression upon *M. humicola* extract exposure. While ablation of AWA neurons[67] showed strong reduction of *chil-27p::GFP* upon exposure to *M. humicola* extract, AWB ablation[68] caused a milder effect. Simultaneous ablation of both neurons did not result in a further reduction in response compared to AWA ablation alone (Figure 3D). We note that the partial *chil-27p::GFP* induction observed in the AWA-ablated strain is likely due to the intestinal expression of *clec-27/35* driving recognition, as simultaneous AWA ablation and intestinal-specific *ceh-37* RNAi resulted in complete loss of *chil-27p::GFP* induction (Figure 3E). This suggests that while AWB neurons possess the capability of contributing to oomycete recognition, neuronal oomycete recognition is predominantly mediated by the AWA neurons.

A different CLEC receptor pair mediates recognition of the phylogenetically divergent oomycete *Haptoglossa zoospora*

It is known that *C. elegans* is able to sense oomycetes that are phylogenetically distinct from *M. humicola*, such as those belonging to the early diverging *Haptoglossa* genus.[48] Therefore, we examined if known regulators of the response to *M. humicola* extract[55] were also relevant for *Haptoglossa zoospora* extract recognition. Surprisingly, we observed strong induction of *chil-27p::GFP* in both *clec-27* and *clec-35* mutants, while there was a strong loss of *chil-27p::GFP* induction in *ceh-37(ok642)*, *old-1(ok1273)*, *flor-1(icb116)*, and *vab-3(icb127)* mutants (Figure 4A). Hence, CLEC-27 and CLEC-35 are not required for *H. zoospora* recognition; however, the required receptor(s) are likely regulated by CEH-37.

To identify if CEH-37-regulated *clecs* are required for *H. zoospora* extract recognition, we performed a targeted RNAi screen focusing on *clec* genes that were found to be downregulated in *ceh-37(ok642)* mutants via RNA-seq (Table S1). In this screen, L4 stage animals carrying the *chil-27p::GFP* reporter were subjected to RNAi targeting CEH-37-regulated *clec* genes before *H. zoospora* extract was added to the plates. Interestingly, only RNAi of *clec-26* and *clec-36* resulted in near complete loss of *chil-27p::GFP* induction upon 48 h of exposure to *H. zoospora* extract (Figure S5A). To consolidate this finding, we generated *clec-26(icb130)*, *clec-36(icb138)*, and *clec-26/36(icb135)* deletion mutants using CRISPR and found loss of *chil-27p::GFP* induction upon exposure to *H. zoospora* extract (Figures 4B and 4C). Conversely, normal induction of *chil-27p::GFP* was observed when *clec-26/36(icb135)* mutants were exposed to *M. humicola* extract (Figure S5B). Intestinal and neuronal expression of *clec-26/36* in *clec-26/36(icb135)* mutants rescued *chil-27p::GFP* induction upon exposure to *H. zoospora* extract (Figures 4C and 4D). Consistent with this result, both neuron-enhanced and intestine-specific RNAi of *clec-26*, *clec-36*, and *ceh-37* strongly reduced *chil-27p::GFP* induction upon exposure to *H. zoospora* extract (Figure S5C).

Like *clec-27/35*, *clec-26* and *clec-36* are neighboring loci on chromosome V and are transcribed in opposite directions; thus, it is likely that they are co-expressed and co-regulated (Figure 4B). A *clec-26/36* transcriptional reporter generated using the shared *clec-26/36* promoter, which also harbors a sequence resembling the OTX2 binding site (Figure S4B), showed GFP and mScarlet co-localization in the head region as well as the intestine (Figure S5D). Interaction between GFP-tagged and myc-tagged CLEC-26 and CLEC-36 was confirmed upon coIP and reverse pull-down in a heterologous eukaryotic expression system (Figure S3). Additionally, we observed co-localization of the *clec-26/36p::mScarlet* transcriptional reporter with the AWA (*odr-10p::GFP*) and AWB (*str-1p::GFP*) neuronal markers (Figure S5E). Rescue of *clec-26/36* expression in AWA or AWB neurons was sufficient to restore *chil-27p::GFP* induction in *clec-26/36(icb135)* mutants upon exposure to *H. zoospora* extract (Figures 4C and 4D). Compared to wild-type animals, AWA-ablated animals displayed a strong reduction in *chil-27p::GFP* induction upon exposure to *H. zoospora* extract,

(F) Loss of *clec-27p::GFP* expression in the anterior body in *ceh-37(ok642)* mutants ($n = 18$, $^{****}p < 0.0001$ based on unpaired t test).
(G) Neuronal (*rab-3p*) and intestinal (*vha-6p*) overexpression of *clec-27/35* in *ceh-37(icb36)* mutant rescue *chil-27p::GFP* induction upon exposure to *M. humicola* extract ($n = 60$ animals, performed in biological triplicates, $^{****}p < 0.0001$ based on chi-squared test).
(H) Quantification of constitutive *chil-27p::GFP* expression upon *old-1* overexpression observed upon *clec-27* and *clec-35* RNAi. RNAi against *gfp* was used as positive control ($n = 50$ per condition, performed in biological triplicates, $^{****}p < 0.0001$ based on chi-squared test).
(I) Quantification of *chil-27p::GFP* induction in *clec-27(icb104)* and *clec-35(icb105)* mutant animals upon *skn-1* and *pals-22* RNAi ($n = 50$, performed in biological triplicates and significance was assessed with chi-squared test). Scale bars in (A) and (B) represent 100 μm and in (F) 25 μm. Error bars in (C), (E), and (G)–(I) represent standard error of proportion. Error bars in (F) represent standard error of mean.

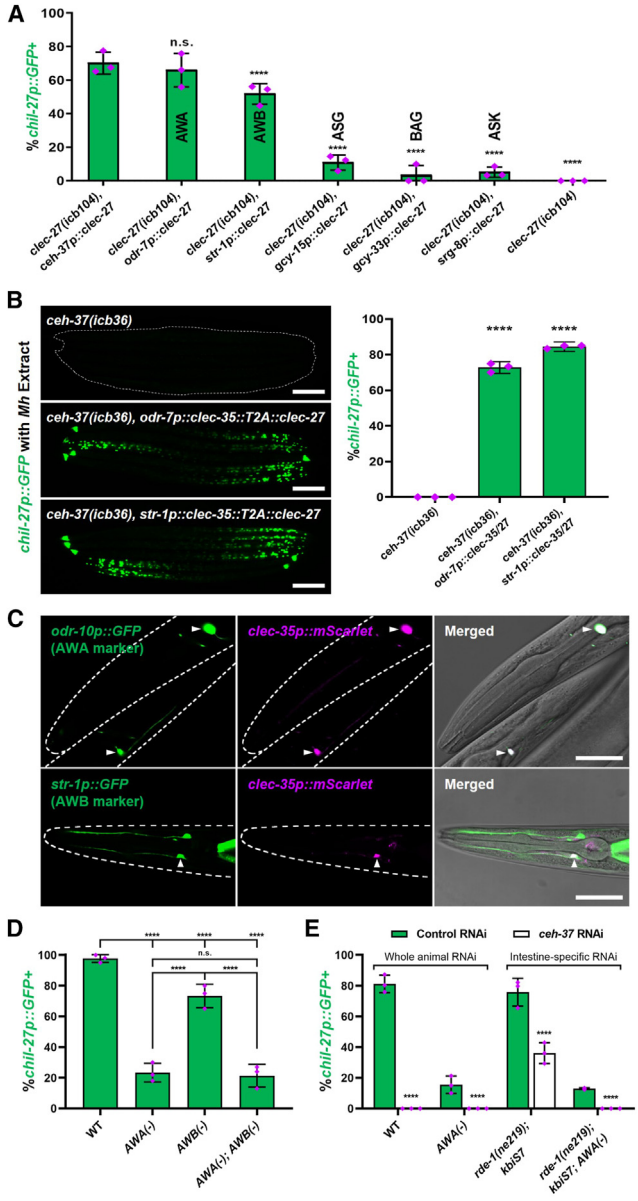


Figure 3. AWA is the main oomycete-sensing neuron

(A) Rescue of *chil-27p::GFP* induction in *clec-27(icb104)* mutants upon *M. humicola* extract treatment by restoring *clec-27* expression in specific neurons. Note that *clec-27* expression in AWA neurons most strongly rescues induction of *chil-27p::GFP* upon *M. humicola* extract exposure, followed by *clec-27* expression in AWB neurons ($n > 60$ animals, performed in biological triplicates, ****$p < 0.0001$ based on Cochran-Mantel-Haenszel test).

(B) AWA-specific (*odr-7p*) and AWB-specific (*str-1p*)expression of *clec-27/35* in *ceh-37(icb36)* is sufficient to rescue induction of *chil-27p::GFP* upon *M. humicola* extract treatment ($n = 60$ animals, performed in biological triplicates, ****$p < 0.0001$ based on chi-squared test).

(C) Co-localization of *clec-35p::mScarlet* with AWA-specific (*odr-10p::GFP*) and AWB-specific (*str-1p::GFP*) markers confirms expression of *clec-27/35* in these neurons (shown with arrows).

(D) Genetic ablation of AWA neurons more strongly reduces *chil-27p::GFP* induction upon exposure to *M. humicola* extract compared to ablation of AWB neurons ($n = 50$ animals, performed in biological triplicates, ****$p < 0.0001$ based on chi-squared test).

(E) AWA ablation combined with intestine-specific RNAi of *ceh-37* leads to complete loss of *chil-27p::GFP* expression ($n = 50$ animals, performed in biological triplicates, ****$p < 0.0001$ based on chi-squared test). Scale bar represents 100 μm in (B) and 25 μm in (C). Error bars in (A) represent standard deviation. Error bars in (B), (D), and (E) represent standard error of proportion.

whereas AWB-ablated animals showed a smaller reduction in *chil-27p::GFP* induction (Figure 4E). Similar to *M. humicola* extract recognition, ablation of both AWA and AWB did not result in further reduction of *chil-27p::GFP* induction compared to AWA ablation alone, suggesting that it is the AWA neurons that primarily mediate neuronal recognition of *H. zoospora*-derived extract (Figure 4E). When genetic ablation of AWA was combined with intestine-specific knockdown of *ceh-37*, we observed complete loss of *chil-27p::GFP* induction upon exposure to *H. zoospora* extract (Figure 4F), highlighting that CLEC-26/36 are likely to act together in sensory neurons and the intestine similar to the CLEC-27/35 pair.

To conclude, our findings demonstrate that selected members of the expanded C-type lectin family in *C. elegans*, physically located next to each other on the genome, can act in pairs to mediate species-specific recognition of divergent oomycete pathogens. Considering the paired genomic organization and the essential requirement for both components of the pair for oomycete recognition, it is plausible that these CLEC proteins function as heterodimeric receptors. It is believed that heterodimerization of CLEC receptors in mammals can increase both the sensitivity for ligands and range of molecules that can be sensed.[69] Our work establishes a paradigm for oomycete recognition wherein canonical pattern recognition receptors act redundantly in non-specialized epithelial and neuronal cells to mount a protective immune response in the skin through cross-tissue communication. Such non-cell autonomous regulation of immunity highlights the complex ways that *C. elegans* can use to sense and respond to its natural eukaryotic pathogens and extends previous reports demonstrating neuronal regulation of host immunity against bacterial infections in *C. elegans*.[7,39,70–72] Activation of CLEC pairs may follow the binding of distinct oomycete-derived ligands and lies upstream of OLD-1/FLOR-1-mediated signaling,[55] which leads to induction of *chil* genes in the epidermis. Interestingly, both the CLEC pair and the OLD-1/FLOR-1 module are regulated by homeodomain proteins (CEH-37 and VAB-3 respectively) known to play broader developmental roles in patterning and sensory organ development,[50,73] and all genes involved in sensing are not induced during infection.[12] We note that among the 283 annotated *clec* genes in the *C. elegans* genome, 28 protein-coding *clec* genes exist in similar pairs sharing a putative bidirectional promoter, 10 of which are also regulated by CEH-37 (Figure 4G). We therefore speculate that other CLEC proteins acting alone or in pairs are likely to play a role in immune response activation against other pathogens, similar to their canonical pattern recognition role in immune detection in mammals.[24]

Limitations of the study

Our study suggests that CLEC-27/35 and CLEC-26/36 form heterodimeric receptor pairs for specific recognition of oomycete pathogens in *C. elegans*. However, we have not directly shown

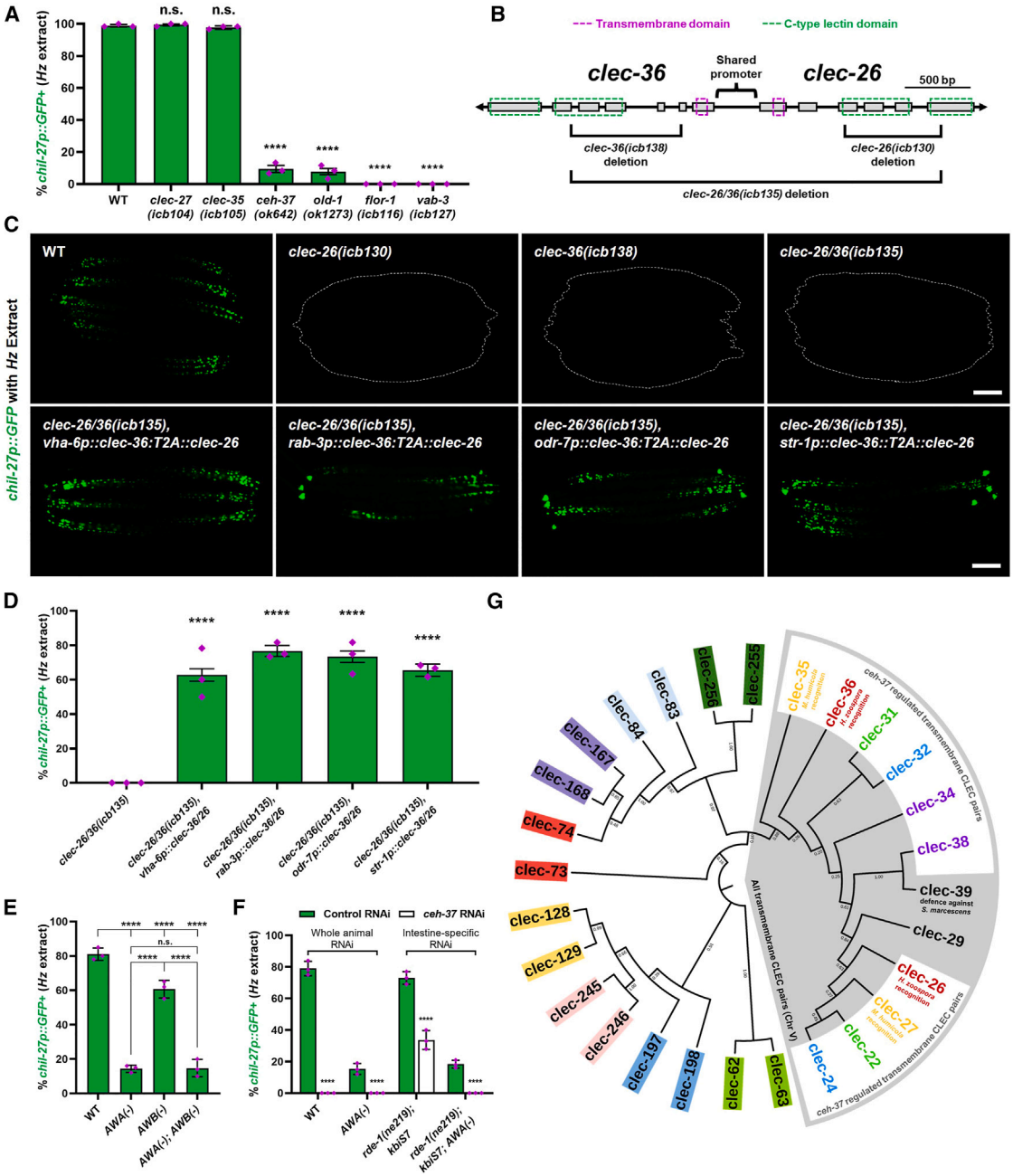


Figure 4. A CLEC-26/36 pair mediates recognition of the oomycete *Haptoglossa zoospora*

(A) Induction of *chil-27p::GFP* in *clec-27(icb104)*, *clec-35(icb105)*, *ceh-37(ok642)*, *old-1(ok1273)*, *flor-1(icb116)*, and *vab-3(icb127)* mutants upon exposure to *H. zoospora* (Hz) extract compared to wild-type animals ($n = 60$ per condition, performed in biological triplicates, $^{****}p < 0.0001$ based on chi-squared test).

(B) Genomic organization of *clec-26* and *clec-36* loci and mutations generated in the study.

(C) Neuronal (*rab-3p*), intestinal (*vha-6p*), AWA-specific (*odr-7p*), and AWB-specific (*str-1p*) expressions of *clec-26/36* are sufficient to rescue *chil-27p::GFP* induction in *clec-26/36(icb135)* mutants upon exposure to *H. zoospora* extract.

(D) Quantification of *chil-27p::GFP* induction in the rescued lines above ($n = 60$ per condition, performed in biological triplicates, $^{****}p < 0.0001$ based on chi-squared test).

(E) Genetic ablation of AWA more strongly reduces *chil-27p::GFP* induction upon exposure to *H. zoospora* extract compared to ablation of AWB neurons ($n = 50$ per condition, performed in biological triplicates, $^{****}p < 0.0001$ based on chi-squared test).

(F) Genetic ablation of AWA combined with intestine-specific knockdown of *ceh-37* significantly compromises induction of *chil-27p::GFP* upon exposure to *H. zoospora* extract ($n = 60$ per condition, performed in biological triplicates, $^{****}p < 0.0001$ based on chi-squared test).

(legend continued on next page)

this interaction in the nematode. While we have shown redundant sensing of the oomycete PAMP in AWA neurons and the intestine, the relative contribution of each of these tissues toward oomycete recognition is yet to be determined. Future work can elucidate the signaling pathway that transmits the signal downstream of CLECs to the epidermis and identify the PAMP(s) enriched in the oomycete extracts that bind to the heterodimeric CLECs for their further validation as oomycete-recognition receptors.

RESOURCE AVAILABILITY

Lead contact

Further information and requests for resources and reagents should be directed to and will be fulfilled by the lead contact, Michalis Barkoulas (m.barkoulas@imperial.ac.uk).

Materials availability

All unique/stable reagents generated in this study are available from the lead contact without restriction.

Data and code availability

- The raw RNA-seq data have been deposited to NCBI GEO under accession GEO: GSE263858.
- All data reported in this paper will be shared by the lead contact upon request.
- This paper does not report original code.
- Any additional information required to re-analyze the data reported in this paper is available from the lead contact upon request.

ACKNOWLEDGMENTS

This work was supported by the Wellcome Trust (219448/Z/19/Z) and BBSRC (BB/X001865/1). We thank Mark Hintze for bioinformatic support and Jonathan Saunders for comments on the manuscript. Some strains were provided by the CGC, which is funded by NIH Office of Research Infrastructure Programs (P40 OD010440). We thank Javier Apfeld for providing the AWA ablation strain and Rachel McMullan for the pRJM163 plasmid (*bus-1p::GFP*). We also thank the Facility for Imaging by Light Microscopy (FILM) at Imperial College London, which is partly supported by funding from the Wellcome Trust (104931/Z/14/Z) and the BBSRC (BB/T017929/1).

AUTHOR CONTRIBUTIONS

K.L. and M.G. conducted most experiments and analyzed the data. F.T. performed the coIP experiment. C.V.-P. and D.I. performed the genetic screens. K.L., M.G., and M.B. wrote the manuscript. All authors edited and approved the final manuscript.

DECLARATION OF INTERESTS

The authors declare no competing interests.

STAR★METHODS

Detailed methods are provided in the online version of this paper and include the following:

- KEY RESOURCES TABLE
- EXPERIMENTAL MODEL AND STUDY PARTICIPANT DETAILS
- METHOD DETAILS
  - EMS mutagenesis
  - Oomycete infection assays
  - *P. aeruginosa* PA14 infection assay
  - RNAseq
  - Microscopy
  - Molecular cloning and transgenesis
  - CRISPR-mediated genome editing
  - RNA interference (RNAi)
  - Single molecule fluorescence *in situ* hybridization
  - Phylogenetic analysis
  - Heterologous *clec* expression and co-immunoprecipitation
- QUANTIFICATION AND STATISTICAL ANALYSIS

SUPPLEMENTAL INFORMATION

Supplemental information can be found online at https://doi.org/10.1016/j.celrep.2024.114906.

Received: June 20, 2024
Revised: September 16, 2024
Accepted: October 8, 2024

REFERENCES

1. Schulenburg, H., and Félix, M.A. (2017). The natural biotic environment of *Caenorhabditis elegans*. Genetics *206*, 55–86. https://doi.org/10.1534/genetics.116.195511.
2. Li, D., and Wu, M. (2021). Pattern recognition receptors in health and diseases. Signal Transduct. Targeted Ther. *6*, 291. https://doi.org/10.1038/s41392-021-00687-0.
3. Martineau, C.N., Kirienko, N.V., and Pujol, N. (2021). Innate immunity in *C. elegans*. Curr. Top. Dev. Biol. *144*, 309–351. https://doi.org/10.1016/bs.ctdb.2020.12.007.
4. Irazoqui, J.E., Urbach, J.M., and Ausubel, F.M. (2010). Evolution of host innate defence: insights from *Caenorhabditis elegans* and primitive invertebrates. Nat. Rev. Immunol. *10*, 47–58. https://doi.org/10.1038/nri2689.
5. Kim, D.H., and Ewbank, J.J. (2018). Signaling in the innate immune response. Worm *2018*, 1–35. https://doi.org/10.1895/wormbook.1.83.2.
6. Pradel, E., Zhang, Y., Pujol, N., Matsuyama, T., Bargmann, C.I., and Ewbank, J.J. (2007). Detection and avoidance of a natural product from the pathogenic bacterium *Serratia marcescens* by *Caenorhabditis elegans*. Proc. Natl. Acad. Sci. USA *104*, 2295–2300. https://doi.org/10.1073/pnas.0610281104.
7. Meisel, J.D., Panda, O., Mahanti, P., Schroeder, F.C., and Kim, D.H. (2014). Chemosensation of bacterial secondary metabolites modulates neuroendocrine signaling and behavior of *C. elegans*. Cell *159*, 267–280. https://doi.org/10.1016/j.cell.2014.09.011.
8. O'Donnell, M.P., Fox, B.W., Chao, P.H., Schroeder, F.C., and Sengupta, P. (2020). A neurotransmitter produced by gut bacteria modulates host sensory behaviour. Nature *583*, 415–420. https://doi.org/10.1038/s41586-020-2395-5.
9. Prakash, D., Ms, A., Radhika, B., Venkatesan, R., Chalasani, S.H., and Singh, V. (2021). 1-Undecene from *Pseudomonas aeruginosa* is an olfactory signal for flight-or-fight response in *Caenorhabditis elegans*. EMBO J. *40*, e106938. https://doi.org/10.15252/embj.2020106938.
10. Wong, D., Bazopoulou, D., Pujol, N., Tavernarakis, N., and Ewbank, J.J. (2007). Genome-wide investigation reveals pathogen-specific and shared

(G) Maximum-likelihood phylogenetic tree using a Jones-Taylor-Thornton model with 500 bootstrap replications showing the relationship between the *clec-27/35* and *clec-26/36* pairs. All paired protein-coding *clec* genes (indicated by the same color) with predicted bidirectional promoters present in the *C. elegans* genome are shown. All *clec* pairs encoding transmembrane proteins are shown within the gray sector, and those that are regulated by CEH-37 are further highlighted in white within the gray sector. Scale bar in (C) represents 100 μm. Error bars in (A) and (D)–(F) represent standard error of proportion.

signatures in the response of *Caenorhabditis elegans* to infection. Genome Biol. *8*, R194. https://doi.org/10.1186/gb-2007-8-9-r194.

11. Irazoqui, J.E., Troemel, E.R., Feinbaum, R.L., Luhachack, L.G., Cezairliyan, B.O., and Ausubel, F.M. (2010). Distinct pathogenesis and host responses during infection of *C. elegans* by *P. aeruginosa* and *S. aureus*. PLoS Pathog. *6*, e1000982. https://doi.org/10.1371/journal.ppat.1000982.
12. Osman, G.A., Fasseas, M.K., Koneru, S.L., Essmann, C.L., Kyrou, K., Srinivasan, M.A., Zhang, G., Sarkies, P., Félix, M.A., and Barkoulas, M. (2018). Natural infection of *C. elegans* by an oomycete reveals a new pathogen-specific immune response. Curr. Biol. *28*, 640–648.e5. https://doi.org/10.1016/j.cub.2018.01.029.
13. Reddy, K.C., Dror, T., Sowa, J.N., Panek, J., Chen, K., Lim, E.S., Wang, D., and Troemel, E.R. (2017). An intracellular pathogen response pathway promotes proteostasis in *C. elegans*. Curr. Biol. *27*, 3544–3553.e5. https://doi.org/10.1016/j.cub.2017.10.009.
14. Yuen, G.J., and Ausubel, F.M. (2018). Both live and dead *Enterococci* activate *Caenorhabditis elegans* host defense via immune and stress pathways. Virulence *9*, 683–699. https://doi.org/10.1080/21505594.2018.1438025.
15. Tran, T.D., and Luallen, R.J. (2024). An organismal understanding of *C. elegans* innate immune responses, from pathogen recognition to multigenerational resistance. Semin. Cell Dev. Biol. *154*, 77–84. https://doi.org/10.1016/j.semcdb.2023.03.005.
16. Brennan, J.J., and Gilmore, T.D. (2018). Evolutionary origins of toll-like receptor signaling. Mol. Biol. Evol. *35*, 1576–1587. https://doi.org/10.1093/molbev/msy050.
17. Schulenburg, H., Kurz, C.L., and Ewbank, J.J. (2004). Evolution of the innate immune system: the worm perspective. Immunol. Rev. *198*, 36–58. https://doi.org/10.1111/j.0105-2896.2004.0125.x.
18. Brandt, J.P., and Ringstad, N. (2015). Toll-like receptor signaling promotes development and function of sensory neurons required for a *C. elegans* pathogen-avoidance behavior. Curr. Biol. *25*, 2228–2237. https://doi.org/10.1016/j.cub.2015.07.037.
19. Pujol, N., Link, E.M., Liu, L.X., Kurz, C., Alloing, G., Tan, M.W., Ray, K.P., Solari, R., Johnson, C.D., and Ewbank, J.J. (2001). A reverse genetic analysis of components of the Toll signaling pathway in *Caenorhabditis elegans*. Curr. Biol. *11*, 809–821. https://doi.org/10.1016/s0960-9822(01)00241-x.
20. Zugasti, O., Bose, N., Squiban, B., Belougne, J., Kurz, C.L., Schroeder, F.C., Pujol, N., and Ewbank, J.J. (2014). Activation of a G protein-coupled receptor by its endogenous ligand triggers the innate immune response of Caenorhabditis elegans. Nat. Immunol. *15*, 833–838. https://doi.org/10.1038/ni.2957.
21. Sowa, J.N., Jiang, H., Somasundaram, L., Tecle, E., Xu, G., Wang, D., and Troemel, E.R. (2020). The *Caenorhabditis elegans* RIG-I homolog DRH-1 mediates the intracellular pathogen response upon viral infection. J. Virol. *94*, e01173-19. https://doi.org/10.1128/JVI.01173-19.
22. Peterson, N.D., Tse, S.Y., Huang, Q.J., Wani, K.A., Schiffer, C.A., and Pukkila-Worley, R. (2023). Non-canonical pattern recognition of a pathogen-derived metabolite by a nuclear hormone receptor identifies virulent bacteria in *C. elegans*. Immunity *56*, 768–782.e9. https://doi.org/10.1016/j.immuni.2023.01.027.
23. Pees, B., Yang, W., Zárate-Potes, A., Schulenburg, H., and Dierking, K. (2016). High innate immune specificity through diversified C-type lectin-Like domain proteins in invertebrates. J. Innate Immun. *8*, 129–142. https://doi.org/10.1159/000441475.
24. Mayer, S., Raulf, M.K., and Lepenies, B. (2017). C-type lectins: their network and roles in pathogen recognition and immunity. Histochem. Cell Biol. *147*, 223–237. https://doi.org/10.1007/s00418-016-1523-7.
25. Brown, G.D., Willment, J.A., and Whitehead, L. (2018). C-type lectins in immunity and homeostasis. Nat. Rev. Immunol. *18*, 374–389. https://doi.org/10.1038/s41577-018-0004-8.
26. Xia, X., You, M., Rao, X.J., and Yu, X.Q. (2018). Insect C-type lectins in innate immunity. Dev. Comp. Immunol. *83*, 70–79. https://doi.org/10.1016/j.dci.2017.11.020.
27. Lu, Y., Su, F., Li, Q., Zhang, J., Li, Y., Tang, T., Hu, Q., and Yu, X.Q. (2020). Pattern recognition receptors in *Drosophila* immune responses. Dev. Comp. Immunol. *102*, 103468. https://doi.org/10.1016/j.dci.2019.103468.
28. Zhang, L., Li, L., Guo, X., Litman, G.W., Dishaw, L.J., and Zhang, G. (2015). Massive expansion and functional divergence of innate immune genes in a protostome. Sci. Rep. *5*, 8693. https://doi.org/10.1038/srep08693.
29. Wang, W., Song, X., Wang, L., and Song, L. (2018). Pathogen-derived carbohydrate recognition in molluscs immune defense. Int. J. Mol. Sci. *19*, 721. https://doi.org/10.3390/ijms19030721.
30. Schulenburg, H., Hoeppner, M.P., Weiner, J., 3rd, and Bornberg-Bauer, E. (2008). Specificity of the innate immune system and diversity of C-type lectin domain (CTLD) proteins in the nematode *Caenorhabditis elegans*. Immunobiology *213*, 237–250. https://doi.org/10.1016/j.imbio.2007.12.004.
31. Engelmann, I., Griffon, A., Tichit, L., Montañana-Sanchis, F., Wang, G., Reinke, V., Waterston, R.H., Hillier, L.W., and Ewbank, J.J. (2011). A comprehensive analysis of gene expression changes provoked by bacterial and fungal infection in *C. elegans*. PLoS One *6*, e19055. https://doi.org/10.1371/journal.pone.0019055.
32. Pees, B., Yang, W., Kloock, A., Petersen, C., Peters, L., Fan, L., Friedrichsen, M., Butze, S., Zárate-Potes, A., Schulenburg, H., and Dierking, K. (2021). Effector and regulator: Diverse functions of *C. elegans* C-type lectin-like domain proteins. PLoS Pathog. *17*, e1009454. https://doi.org/10.1371/journal.ppat.1009454.
33. Boehnisch, C., Wong, D., Habig, M., Isermann, K., Michiels, N.K., Roeder, T., May, R.C., and Schulenburg, H. (2011). Protist-type lysozymes of the nematode *Caenorhabditis elegans* contribute to resistance against pathogenic *Bacillus thuringiensis*. PLoS One *6*, e24619. https://doi.org/10.1371/journal.pone.0024619.
34. Shapira, M., Hamlin, B.J., Rong, J., Chen, K., Ronen, M., and Tan, M.W. (2006). A conserved role for a GATA transcription factor in regulating epithelial innate immune responses. Proc. Natl. Acad. Sci. USA *103*, 14086–14091. https://doi.org/10.1073/pnas.0603424103.
35. Pan, W., Huang, X., Guo, Z., Nagarajan, R., and Mylonakis, E. (2021). Identification and functional analysis of cytokine-like protein CLEC-47 in *Caenorhabditis elegans*. mBio *12*, e0257921. https://doi.org/10.1128/mBio.02579-21.
36. O'Rourke, D., Baban, D., Demidova, M., Mott, R., and Hodgkin, J. (2006). Genomic clusters, putative pathogen recognition molecules, and antimicrobial genes are induced by infection of *C. elegans* with *M. nematophilum*. Genome Res. *16*, 1005–1016. https://doi.org/10.1101/gr.50823006.
37. Sahu, S.N., Lewis, J., Patel, I., Bozdag, S., Lee, J.H., LeClerc, J.E., and Cinar, H.N. (2012). Genomic analysis of immune response against *Vibrio cholerae* hemolysin in *Caenorhabditis elegans*. PLoS One *7*, e38200. https://doi.org/10.1371/journal.pone.0038200.
38. Miltsch, S.M., Seeberger, P.H., and Lepenies, B. (2014). The C-type lectin-like domain containing proteins CLEC-39 and CLEC-49 are crucial for *Caenorhabditis elegans* immunity against *Serratia marcescens* infection. Dev. Comp. Immunol. *45*, 67–73. https://doi.org/10.1016/j.dci.2014.02.002.
39. Wibisono, P., Wibisono, S., Watteyne, J., Chen, C.H., Sellegounder, D., Beets, I., Liu, Y., and Sun, J. (2022). Neuronal GPCR NMUR-1 regulates distinct immune responses to different pathogens. Cell Rep. *38*, 110321. https://doi.org/10.1016/j.celrep.2022.110321.
40. Simonsen, K.T., Møller-Jensen, J., Kristensen, A.R., Andersen, J.S., Riddle, D.L., and Kallipolitis, B.H. (2011). Quantitative proteomics identifies ferritin in the innate immune response of *C. elegans*. Virulence *2*, 120–130. https://doi.org/10.4161/viru.2.2.15270.
41. Gallotta, I., Sandhu, A., Peters, M., Haslbeck, M., Jung, R., Agilkaya, S., Blersch, J.L., Rödelsperger, C., Röseler, W., Huang, C., et al. (2020).

Extracellular proteostasis prevents aggregation during pathogenic attack. Nature *584*, 410–414. https://doi.org/10.1038/s41586-020-2461-z.

42. Pees, B., Kloock, A., Nakad, R., Barbosa, C., and Dierking, K. (2017). Enhanced behavioral immune defenses in a *C. elegans* C-type lectin-like domain gene mutant. Dev. Comp. Immunol. *74*, 237–242. https://doi.org/10.1016/j.dci.2017.04.021.
43. Drickamer, K., and Dodd, R.B. (1999). C-Type lectin-like domains in *Caenorhabditis elegans*: predictions from the complete genome sequence. Glycobiology *9*, 1357–1369. https://doi.org/10.1093/glycob/9.12.1357.
44. Yunger, E., Safra, M., Levi-Ferber, M., Haviv-Chesner, A., and Henis-Korenblit, S. (2017). Innate immunity mediated longevity and longevity induced by germ cell removal converge on the C-type lectin domain protein IRG-7. PLoS Genet. *13*, e1006577. https://doi.org/10.1371/journal.pgen.1006577.
45. Kulkarni, G., Li, H., and Wadsworth, W.G. (2008). CLEC-38, a transmembrane protein with C-type lectin-like domains, negatively regulates UNC-40-mediated axon outgrowth and promotes presynaptic development in *Caenorhabditis elegans*. J. Neurosci. *28*, 4541–4550. https://doi.org/10.1523/JNEUROSCI.5542-07.2008.
46. Wang, J., Wang, D., Setrerrahmane, S., Martinez, J., and Xu, H.M. (2023). The peptide Acein promotes dopamine secretion through *clec-126* to extend the lifespan of elderly *C. elegans*. Aging (Albany NY) *15*, 14651–14665. https://doi.org/10.18632/aging.205150.
47. Grover, M., and Barkoulas, M. (2021). *C. elegans* as a new tractable host to study infections by animal pathogenic oomycetes. PLoS Pathog. *17*, e1009316. https://doi.org/10.1371/journal.ppat.1009316.
48. Grover, M., Fasseas, M.K., Essmann, C., Liu, K., Braendle, C., Félix, M.A., Glockling, S.L., and Barkoulas, M. (2021). Infection of *C. elegans* by *Haptoglossa* species reveals shared features in the host response to oomycete detection. Front. Cell. Infect. Microbiol. *11*, 733094. https://doi.org/10.3389/fcimb.2021.733094.
49. Fasseas, M.K., Grover, M., Drury, F., Essmann, C.L., Kaulich, E., Schafer, W.R., and Barkoulas, M. (2021). Chemosensory neurons modulate the response to oomycete recognition in *Caenorhabditis elegans*. Cell Rep. *34*, 108604. https://doi.org/10.1016/j.celrep.2020.108604.
50. Lanjuin, A., VanHoven, M.K., Bargmann, C.I., Thompson, J.K., and Sengupta, P. (2003). Otx/otd homeobox genes specify distinct sensory neuron identities in *C. elegans*. Dev. Cell *5*, 621–633. https://doi.org/10.1016/s1534-5807(03)00293-4.
51. Moon, S., Lee, Y.W., Kim, W.T., and Lee, W. (2014). Solution structure of CEH-37 homeodomain of the nematode *Caenorhabditis elegans*. Biochem. Biophys. Res. Commun. *443*, 370–375. https://doi.org/10.1016/j.bbrc.2013.11.133.
52. Kim, S.H., Hwang, S.B., Chung, I.K., and Lee, J. (2003). Sequence-specific binding to telomeric DNA by CEH-37, a homeodomain protein in the nematode *Caenorhabditis elegans*. J. Biol. Chem. *278*, 28038–28044. https://doi.org/10.1074/jbc.M302192200.
53. Liu, F., Zhang, H., Wang, H., Zhu, X., Li, S., Jiang, N., Yu, C., Liu, Y., and Xiao, Y. (2023). The homeodomain transcription factor CEH-37 regulates PMK-1/p38 MAPK pathway to protect against intestinal infection via the phosphatase VHP-1. Cell. Mol. Life Sci. *80*, 312. https://doi.org/10.1007/s00018-023-04970-x.
54. C elegans Deletion Mutant Consortium (2012). large-scale screening for targeted knockouts in the Caenorhabditis elegans genome. G3 (Bethesda) *2*, 1415–1425. https://doi.org/10.1534/g3.112.003830.
55. Drury, F., Grover, M., Hintze, M., Saunders, J., Fasseas, M.K., Constantinou, C., and Barkoulas, M. (2023). A PAX6-regulated receptor tyrosine kinase pairs with a pseudokinase to activate immune defense upon oomycete recognition in *Caenorhabditis elegans*. Proc. Natl. Acad. Sci. USA *120*, e2300587120. https://doi.org/10.1073/pnas.2300587120.
56. Reilly, M.B., Cros, C., Varol, E., Yemini, E., and Hobert, O. (2020). Unique homeobox codes delineate all the neuron classes of *C. elegans*. Nature *584*, 595–601. https://doi.org/10.1038/s41586-020-2618-9.
57. Buecker, C., Srinivasan, R., Wu, Z., Calo, E., Acampora, D., Faial, T., Simeone, A., Tan, M., Swigut, T., and Wysocka, J. (2014). Reorganization of enhancer patterns in transition from naive to primed pluripotency. Cell Stem Cell *14*, 838–853. https://doi.org/10.1016/j.stem.2014.04.003.
58. Grover, M., Gang, S.S., Troemel, E.R., and Barkoulas, M. (2024). Proteasome inhibition triggers tissue-specific immune responses against different pathogens in *C. elegans*. PLoS Biol. *22*, e3002543. https://doi.org/10.1371/journal.pbio.3002543.
59. Reddy, K.C., Dror, T., Underwood, R.S., Osman, G.A., Elder, C.R., Desjardins, C.A., Cuomo, C.A., Barkoulas, M., and Troemel, E.R. (2019). Antagonistic paralogs control a switch between growth and pathogen resistance in *C. elegans*. PLoS Pathog. *15*, e1007528. https://doi.org/10.1371/journal.ppat.1007528.
60. Gang, S.S., Grover, M., Reddy, K.C., Raman, D., Chang, Y.T., Ekiert, D.C., Barkoulas, M., and Troemel, E.R. (2022). A *pals-25* gain-of-function allele triggers systemic resistance against natural pathogens of C. elegans. PLoS Genet. *18*, e1010314. https://doi.org/10.1371/journal.pgen.1010314.
61. Colosimo, M.E., Tran, S., and Sengupta, P. (2003). The divergent orphan nuclear receptor ODR-7 regulates olfactory neuron gene expression via multiple mechanisms in *Caenorhabditis elegans*. Genetics *165*, 1779–1791. https://doi.org/10.1093/genetics/165.4.1779.
62. Troemel, E.R., Kimmel, B.E., and Bargmann, C.I. (1997). Reprogramming chemotaxis responses: sensory neurons define olfactory preferences in *C. elegans*. Cell *91*, 161–169. https://doi.org/10.1016/s0092-8674(00)80399-2.
63. Ortiz, C.O., Etchberger, J.F., Posy, S.L., Frøkjaer-Jensen, C., Lockery, S., Honig, B., and Hobert, O. (2006). Searching for neuronal left/right asymmetry: genomewide analysis of nematode receptor-type guanylyl cyclases. Genetics *173*, 131–149. https://doi.org/10.1534/genetics.106.055749.
64. Yu, S., Avery, L., Baude, E., and Garbers, D.L. (1997). Guanylyl cyclase expression in specific sensory neurons: a new family of chemosensory receptors. Proc. Natl. Acad. Sci. USA *94*, 3384–3387. https://doi.org/10.1073/pnas.94.7.3384.
65. Troemel, E.R., Chou, J.H., Dwyer, N.D., Colbert, H.A., and Bargmann, C.I. (1995). Divergent seven transmembrane receptors are candidate chemosensory receptors in *C. elegans*. Cell *83*, 207–218. https://doi.org/10.1016/0092-8674(95)90162-0.
66. Sengupta, P., Chou, J.H., and Bargmann, C.I. (1996). *odr-10* encodes a seven transmembrane domain olfactory receptor required for responses to the odorant diacetyl. Cell *84*, 899–909. https://doi.org/10.1016/s0092-8674(00)81068-5.
67. Schiffer, J.A., Servello, F.A., Heath, W.R., Amrit, F.R.G., Stumbur, S.V., Eder, M., Martin, O.M., Johnsen, S.B., Stanley, J.A., Tam, H., et al. (2020). *Caenorhabditis elegans* processes sensory information to choose between freeloading and self-defense strategies. Elife *9*, e56186. https://doi.org/10.7554/eLife.56186.
68. Yoshida, K., Hirotsu, T., Tagawa, T., Oda, S., Wakabayashi, T., Iino, Y., and Ishihara, T. (2012). Odour concentration-dependent olfactory preference change in *C. elegans*. Nat. Commun. *3*, 739. https://doi.org/10.1038/ncomms1750.
69. Zhu, L.L., Zhao, X.Q., Jiang, C., You, Y., Chen, X.P., Jiang, Y.Y., Jia, X.M., and Lin, X. (2013). C-type lectin receptors Dectin-3 and Dectin-2 form a heterodimeric pattern-recognition receptor for host defense against fungal infection. Immunity *39*, 324–334. https://doi.org/10.1016/j.immuni.2013.05.017.
70. Wani, K.A., Goswamy, D., and Irazoqui, J.E. (2020). Nervous system control of intestinal host defense in *C. elegans*. Curr. Opin. Neurobiol. *62*, 1–9. https://doi.org/10.1016/j.conb.2019.11.007.
71. Sellegounder, D., Liu, Y., Wibisono, P., Chen, C.H., Leap, D., and Sun, J. (2019). Neuronal GPCR NPR-8 regulates *C. elegans* defense against pathogen infection. Sci. Adv. *5*, eaaw4717. https://doi.org/10.1126/sciadv.aaw4717.

72. Foster, K.J., Cheesman, H.K., Liu, P., Peterson, N.D., Anderson, S.M., and Pukkila-Worley, R. (2020). Innate Immunity in the *C. elegans* intestine is programmed by a neuronal regulator of AWC olfactory neuron development. Cell Rep. *31*, 107478. https://doi.org/10.1016/j.celrep.2020.03.042.

73. Chisholm, A.D., and Horvitz, H.R. (1995). Patterning of the *Caenorhabditis elegans* head region by the Pax-6 family member *vab-3*. Nature *377*, 52–55. https://doi.org/10.1038/377052a0.

74. Yuen, E.L.H., Leary, A.Y., Clavel, M., Tumtas, Y., Mohseni, A., Zhao, J., Picchianti, L., Jamshidiha, M., Pandey, P., Duggan, C., et al. (2024). A RabGAP negatively regulates plant autophagy and immune trafficking. Curr. Biol. *34*, 2049–2065.e6. https://doi.org/10.1016/j.cub.2024.04.002.

75. Schindelin, J., Arganda-Carreras, I., Frise, E., Kaynig, V., Longair, M., Pietzsch, T., Preibisch, S., Rueden, C., Saalfeld, S., Schmid, B., et al. (2012). Fiji: an open-source platform for biological-image analysis. Nat. Methods *9*, 676–682. https://doi.org/10.1038/nmeth.2019.

76. Bray, N.L., Pimentel, H., Melsted, P., and Pachter, L. (2016). Near-optimal probabilistic RNA-seq quantification. Nat. Biotechnol. *34*, 525–527. https://doi.org/10.1038/nbt.3519.

77. Han, S.K., Lee, D., Lee, H., Kim, D., Son, H.G., Yang, J.S., Lee, S.J.V., and Kim, S. (2016). OASIS 2: online application for survival analysis 2 with features for the analysis of maximal lifespan and healthspan in aging research. Oncotarget *7*, 56147–56152. https://doi.org/10.18632/oncotarget.11269.

78. Tamura, K., Stecher, G., and Kumar, S. (2021). MEGA11: Molecular evolutionary genetics analysis version 11. Mol. Biol. Evol. *38*, 3022–3027. https://doi.org/10.1093/molbev/msab120.

79. Stiernagle, T. (2006). Maintenance of *C. elegans* (WormBook), pp. 1–11. https://doi.org/10.1895/wormbook.1.101.1.

80. Minevich, G., Park, D.S., Blankenberg, D., Poole, R.J., and Hobert, O. (2012). CloudMap: a cloud-based pipeline for analysis of mutant genome sequences. Genetics *192*, 1249–1269. https://doi.org/10.1534/genetics.112.144204.

81. Pimentel, H., Bray, N.L., Puente, S., Melsted, P., and Pachter, L. (2017). Differential analysis of RNA-seq incorporating quantification uncertainty. Nat. Methods *14*, 687–690. https://doi.org/10.1038/nmeth.4324.

82. Timmons, L., Court, D.L., and Fire, A. (2001). Ingestion of bacterially expressed dsRNAs can produce specific and potent genetic interference in *Caenorhabditis elegans*. Gene *263*, 103–112. https://doi.org/10.1016/s0378-1119(00)00579-5.

83. Hintze, M., Koneru, S.L., Gilbert, S.P.R., Katsanos, D., Lambert, J., and Barkoulas, M. (2020). A cell fate switch in the *Caenorhabditis elegans* seam cell lineage occurs through modulation of the Wnt asymmetry pathway in response to temperature increase. Genetics *214*, 927–939. https://doi.org/10.1534/genetics.119.302896.

STAR★METHODS

KEY RESOURCES TABLE

REAGENT or RESOURCE	SOURCE	IDENTIFIER
Antibodies		
α-GFP, rabbit	Invitrogen	Cat# A11122; RRID: AB_221569
α-myc, rat	Proteintech	Cat# 9E1; RRID: AB_2631398
HRP-coupled antibody, α-rabbit	Merck	Cat# A9169; RRID: AB_258434
HRP-coupled antibody, α-rat	Merck	Cat# A9037; RRID: AB_258429
Bacterial and virus strains		
E. coli OP50	Caenorhabditis Genetics Center	Wormbase ID: OP50
Ahringer RNAi Library in *E. coli* HT115	Source Bioscience	N/A
C. elegans ORFeome (Vidal RNAi Library) in *E. coli* HT115	Horizon Discovery	N/A
A. tumefaciens GV3101	Tolga Bozkurt Lab Collection (Yuen et al., 2024)[74]	N/A
Chemicals, peptides, and recombinant proteins		
Ethyl methanesulfonate (EMS)	Sigma	Ca# M0880
Isopropyl β- d-1-thiogalactopyranoside (IPTG)	Thermo Scientific	Cat# R0392
TRIzol	Invitrogen	Cat# 15596026
Critical commercial assays		
QIAquick PCR Purification Kit	Qiagen	Cat# 28106
PureLink Quick Gel Extraction Kit	Invitrogen	Cat# K210012
PureLink Quick Plasmid Miniprep Kit	Invitrogen	Cat# K210011
Deposited data		
RNA-seq data, normalized per gene sequence counts and differentially expressed genes as determined by Kallisto & Sleuth respectively	This Paper	GEO: GSE263858
Experimental models: Organisms/strains		
Myzocytiopsis humicola (Lisbon Isolate)	Osman et al., 2018[12]	JUo1
Haptoglossa zoospora (Eastbourne Isolate)	Grover et al., 2021[48]	MBAo1
Nicotiana benthamiana (wildtype)	Tolga Bozkurt Lab Collection (Yuen et al., 2024)[74]	N/A
C. elegans: wild-type N2	Caenorhabditis Genetics Center	Wormbase ID: N2
C. elegans: icbIs4[pGO4, pCMH1195] II	Osman et al., 2018[12]	MBA281
C. elegans: icbIs5[pGO4, pCMH1195] IV	Osman et al., 2018[12]	MBA282
C. elegans: ceh-37(ok642) X	Caenorhabditis Genetics Center	LJ2
C. elegans: icbIs4[pGO4, pCMH1195] II; ceh-37(icb36) X	This study	MBA503
C. elegans: icbIs4[pGO4, pCMH1195] II; ceh-37(ok642) X	This study	MBA1054
C. elegans: icbIs4[pGO4, pCMH1195] II; ceh-37(icb159) X	This study	MBA1700
C. elegans: icbIs4[pGO4, pCMH1195] II; ceh-37(icb152) X	This study	MBA1702
C. elegans: icbIs4[pGO4, pCMH1195] II; clec-35(icb153) V	This study	MBA1703
C. elegans: icbIs4[pGO4, pCMH1195] II; clec-35(icb150) V	This study	MBA1697
C. elegans: icbIs4[pGO4, pCMH1195] II; clec-35(icb105) V	This study	MBA1105
C. elegans: icbIs4[pGO4, pCMH1195] II; clec-27(icb104) V	This study	MBA1104
C. elegans: icbIs4[pGO4, pCMH1195] II; clec-27(icb147) V	This study	MBA1693

(*Continued on next page*)

Continued

REAGENT or RESOURCE	SOURCE	IDENTIFIER
C. elegans: icbIs4[pGO4, pCMH1195] II; clec-27(icb104) V; icbEx293[clec-27p::clec-27, bus-1p::GFP, pBJ36]	This study	MBA1116
C. elegans: icbIs4[pGO4, pCMH1195] II; clec-35(icb105) V; icbEx296[clec-35p::clec-35, bus-1p::GFP, pBJ36]	This study	MBA1119
C. elegans: icbEx636[ceh-37(WRM065bE05), bus-1p::GFP, pBJ36], icbIs4[pGO4, pCMH1195] II; ceh-37(icb36) X	This study	MBA1785
C. elegans: clec-27(icb104) V	This study	MBA1130
C. elegans: clec-35(icb105) V	This study	MBA1111
C. elegans: icbEx306[pCV12(clec-35 3′UTR:wrmscarlet::clec-35/27p::GFPo::clec-27 3′UTR), bus-1p::GFP]	This study	MBA1199
C. elegans: icbIs4[pGO4, pCMH1195] II; clec-35(icb105) V; icbEx634[pCV10(rab-3p::clec-35::T2A::clec-27), bus-1p::GFP, pBJ36]	This study	MBA1208
C. elegans: icbIs4[pGO4, pCMH1195] II; clec-35(icb105) V; icbEx635[pCV11(dpy-7p::clec-35::T2A::clec-27), bus-1p::GFP, pBJ36]	This study	MBA1783
C. elegans: icbIs4[pGO4, pCMH1195] II; clec-35 (icb105) V; icbEx658[pKL158(vha-6p::clec-35::T2A::clec-27), bus-1p::GFP, pBJ36]	This study	MBA1877
C. elegans: ceh-37(ok642) X; icbEx306[pCV12(clec-35 3′UTR:wrmscarlet::clec-35/27p::GFPo::clec-27 3′UTR), bus-1p::GFP, pBJ36]	This study	MBA1906
C. elegans: icbIs4[pGO4, pCMH1195] II; ceh-37(icb36) X; icbEX686[pKL158(vha-6p::clec-35::T2A::clec-27), bus-1p::GFP, pBJ36]	This study	MBA1918
C. elegans: icbEx634[pCV10(rab-3p::clec-35::T2A::clec-27), bus-1p::GFP, pBJ36], icbIs4[pGO4, pCMH1195]II; ceh-37(icb36) X	This study	MBA1784
C. elegans: icbIs4[pGO4, pCMH1195] II; clec-27(icb104) V; icbEx329[pKL1(srg-8p::clec-27), bus-1p::GFP, pBJ36]	This study	MBA1298
C. elegans: icbIs4[pGO4, pCMH1195] II; clec-27(icb104) V; icbEx330[pKL2(gcy-15p::clec-27), bus-1p::GFP, pBJ36]	This study	MBA1232
C. elegans: icbIs4[pGO4, pCMH1195] II; clec-27(icb104) V; icbEx331[pKL3(gcy-33p::clec-27), bus-1p::GFP, pBJ36]	This study	MBA1233
C. elegans: icbIs4[pGO4, pCMH1195] II; clec-27(icb104) V; icbEx332[pKL4(str-1p::clec-27), bus-1p::GFP, pBJ36]	This study	MBA1234
C. elegans: icbIs4[pGO4, pCMH1195] II; clec-27(icb104) V; icbEx337[pKL6(ceh-37p::clec-27), bus-1p::GFP, pBJ36]	This study	MBA1301
C. elegans: icbIs4[pGO4, pCMH1195] II; clec-27(icb104) V; icbEx339[pKL7(odr-7p::clec-27), bus-1p::GFP, pBJ36]	This study	MBA1302
C. elegans: icbIs4[pGO4, pCMH1195] II; ceh-37(icb36) X; icbEx345[pKL8(odr-7p::clec-35::T2A::clec-27), bus-1p::GFP, pBJ36]	This study	MBA1306
C. elegans: icbIs4[pGO4, pCMH1195] II; ceh-37(icb36) X; icbEx595[pKL128(str-1p::clec-35::T2A::clec-27), bus-1p::GFP, pBJ36]	This study	MBA1732

(*Continued on next page*)

Continued

REAGENT or RESOURCE	SOURCE	IDENTIFIER
C. elegans: icbEx450[pKL53(odr-10p::GFP), PIP1303F(rpsa-1p::hgb:unc-54), pBJ36]; icbEx515[pKL71(clec-35p::wrmscarlet), bus-1p::GFP, pBJ36]	This study	MBA1864
C. elegans: icbEx451[pKL54(str-1p::GFP), PIP1303F(rpsa-1p::hgb:unc-54), pBJ36]; icbEx515[pKL71(clec-35p::wrmScarlet), bus-1p::GFP, pBJ36]	This study	MBA1598
C. elegans: icbIs4[pGO4, pCMH1195] II; Ex[odr-10::mCasp1, myo-3::GFP]	This study	MBA1754
C. elegans: icbIs4[pGO4, pCMH1195] II; peIs1715[str-1::mCasp1 + unc-122::GFP]; Ex[odr-10::mCasp1, myo-3::GFP]	This study	MBA1755
C. elegans: peIs1715[str-1p::mCasp-1, unc-122p::GFP], icbIs4[pGO4, pCMH1195] II	Fasseas et al., 2021[49]	MBA1196
C. elegans: kbIs7[nhx-2p::rde-1]; rol-6(su1006) II; icbIs5[pGO4, pCMH1195] IV; rde-1(ne219) V	Grover et al., 2024[58]	MBA597
C. elegans: kbIs7[nhx-2p::rde-1]; rol-6(su1006) II; icbIs5[pGO4, pCMH1195] IV; rde-1(ne219) V; Ex[odr-10::mCasp1 + myo-3::GFP]	This study	MBA1907
C. elegans: old-1(ok1273) II; icbIs4[pGO4, pCMH1195] IV	Drury et al., 2023[55]	MBA1018
C. elegans: icbIs4[pGO4, pCMH1195] IV; flor-1(icb116) V	Drury et al., 2023[55]	MBA1415
C. elegans: icbIs22[old-1p::old-1, bus-1p::GFP, pBJ36] IV; icbIs5[pGO4, pCMH1195] IV; vab-3(icb127) X	Drury et al., 2023[55]	MBA1339
C. elegans: icbIs4[pGO4, pCMH1195] II; clec-26(icb130) V	This study	MBA1472
C. elegans: icbIs4[pGO4, pCMH1195] II; clec-36(icb138) V	This study	MBA1605
C. elegans: icbIs4[pGO4, pCMH1195] II; clec-26/36(icb135) V	This study	MBA1578
C. elegans: icbIs4[pGO4, pCMH1195] II; clec-26/36 (icb135) V; icbEx619[pKL136(rab-3p::clec-36::GSG-T2A::clec-26), bus-1p::GFP, pBJ36]	This study	MBA1791
C. elegans: icbIs4[pGO4, pCMH1195] II; clec-26/36 (icb135) V; icbEx505[pKL63(odr-7p::clec-36::GSG-T2A::clec-26), bus-1p::GFP, pBJ36]	This study	MBA1577
C. elegans: icbIs4[pGO4, pCMH1195] II; clec-26/36(icb135) V; icbEx597[pKL130(str-1p::clec-36::T2A::clec-26), bus-1p::GFP, pBJ36]	This study	MBA1734
C. elegans: icbIs4[pGO4, pCMH1195] II; clec-26/36 (icb135) V; icbEx624[pKL141(vha-6p::clec-36::T2A::clec-26), bus-1p::GFP, pBJ36]	This study	MBA1796
C. elegans: icbIs4[pGO4, pCMH1195] II; sid-1(pk3321) uIs69 V	Grover et al., 2024[58]	MBA501
C. elegans: icbIs5[pGO4, pCMH1195] IV; rde-1(ne219) V; xkIs99 [wrt-2p::rde-1::unc-54 3′UTR]	Drury et al., 2023[55]	MBA576
C. elegans: ceh-37(ot1023[ceh-37::GFP::FLAG]) X.	Caenorhabditis Genetics Center	OH16345
C. elegans: icbIs22[old-1p::old-1::GFP, bus-1p::GFP, pBJ36] IV; icbIs5[pGO4, pCMH1195] IV;	Drury et al., 2023[55]	MBA1437
C. elegans: icbEx449 [pKL52(wrmScarlet::clec-26/36p::GFP), bus-1p::GFP, pBJ36]	This study	MBA1477
C. elegans: icbEx450 [pKL53(odr-10p::GFP), PIP1303F(rpsa-1p::hgb:unc-54), pBJ36] icbEx516[pKL72(clec-36p::wrmScarlet), bus-1p::GFP, pBJ36]	This study	MBA1599
C. elegans: icbEx450 [pKL54(str-1p::GFP), PIP1303F(rpsa-1p::hgb:unc-54), pBJ36]; icbEx516[pKL72(clec-36p::wrmScarlet), bus-1p::GFP, pBJ36]	This study	MBA1919

(*Continued on next page*)

Continued

REAGENT or RESOURCE	SOURCE	IDENTIFIER
C. elegans: icbIs4[pGO4, pCMH1195] II; clec-35(icb105) V; icbEx756[clec-27p::clec-27, bus-1p::GFP, pBJ36]	This study	MBA2088
C. elegans: icbIs4[pGO4, pCMH1195] II; clec-27(icb104) V; icbEx757[clec-35p::clec-35, bus-1p::GFP, pBJ36]	This study	MBA2089
Oligonucleotides		
See Table S2 for the list of oligonucleotides used	–	–
Recombinant DNA		
Plasmid: *clec-35 3′UTR:wrmscarlet::clec-35/27p::GFPo:: clec-27 3′UTR* (in pUC57)	Genewiz	pCV12
Plasmid: *rab-3p::clec-35::T2A::clec-27::unc-54 3′UTR* (in pBJ97)	This study	pCV10
Plasmid: *dpy-7p::clec-35::T2A::clec-27::unc-54 3′UTR* (in pUC57)	This study	pCV11
Plasmid: *vha-6p::clec-35::T2A::clec-27::unc-54 3′UTR* (in pBJ97)	This study	pKL158
Plasmid: *srg-8p::clec-27::clec-27 3′UTR* (in pBJ97)	This study	pKL1
Plasmid: *gcy-15p::clec-27::clec-27 3′UTR* (in pBJ97)	This study	pKL2
Plasmid: *gcy-33p::clec-27::clec-27 3′UTR* (in pBJ97)	This study	pKL3
Plasmid: *str-1p::clec-27::clec-27 3′UTR* (in pBJ97)	This study	pKL4
Plasmid: *ceh-37p::clec-27::clec-27 3′UTR* (in pBJ97)	This study	pKL6
Plasmid: *odr-10p::clec-27::clec-27 3′UTR* (in pBJ97)	This study	pKL7
Plasmid: *odr-7p::clec-35::T2A::clec-27::unc-54 3′UTR* (in pBJ97)	This study	pKL8
Plasmid: *str-1::clec-35::T2A::clec-27::unc-54 3′UTR* (in pBJ97)	This study	pKL128
Plasmid: *odr-10p::GFPo::unc-54 3′UTR* (in pBJ97)	This study	pKL53
Plasmid: *str-1p::GFPo::unc-54 3′UTR* (in pBJ97)	–	pKL54
Plasmid: *clec-36 3′UTR:wrmscarlet::clec-36/26p::GFPo:: clec-26 3′UTR* (in pUC-GW-AMP)	Genewiz	N/A
Plasmid: *vha-6p::clec-36::T2A::clec-26::unc-54 3′UTR* (in pBJ97)	This study	pKL141
Plasmid: *rab-3p::clec-36::T2A::clec-26::unc-54 3′UTR* (in pBJ97)	This study	pKL136
Plasmid: *odr-7p::clec-36::T2A::clec-26::unc-54 3′UTR* (in pBJ97)	This study	pKL63
Plasmid: *str-1p::clec-36::T2A::clec-26::unc-54 3′UTR* (in pBJ97)	This study	pKL130
Software and algorithms		
GraphPad Prism 7	GraphPad Software, La Jolla, CA	https://www.graphpad.com/scientificsoftware/prism/
Fiji	Schindelin et al., 2012[75]	https://imagej.net/software/fiji/
Kallisto	Bray et al., 2016[76]	https://pachterlab.github.io/kallisto/
OASIS 2	Han et al., 2016[77]	https://sbi.postech.ac.kr/oasis2/
MEGA 11	Tamura et al., 2021[78]	https://www.megasoftware.net/

EXPERIMENTAL MODEL AND STUDY PARTICIPANT DETAILS

All *C. elegans* strains were cultured on NGM plates seeded with *E. coli* OP50, at 20°C under standard conditions as previously described.[79] Continuous cultures of oomycete isolates were maintained by chunking infected animals on an OP50-NGM plate whenever the plate was running out of food with intermittent addition of fresh N2.[12,48] The list of all the strains used in this study is available in the supplementary Table S2.

METHOD DETAILS

EMS mutagenesis

L4 stage animals carrying the *chil-27p::GFP* reporter were mutagenized with 24 mM ethyl methanesulfonate (EMS) (Sigma) in 4 mL M9, for 4 h with intermittent mixing by inversion. Mutagenised animals were then washed 10 times with 15 mL M9 to completely get rid of EMS from the suspension and plated onto 90 mm NGM plates seeded with *E. coli* OP50. After brief recovery (4-12h), adults were randomly picked and divided into 90 mm plates carrying 10 animals in each. After 72 h at 20°C, all F1 gravid adults in each plate were individually bleached and respective pool of F2 embryos were collected onto new plates containing *M. humicola* extract prepared as

previously described.[49] Around 120,000 haploid genomes were screened in multiple independent screens to identify animals showing loss of *chil-27p::GFP* induction upon extract treatment. The causative mutations *ceh-37(icb36)*, *clec-27(icb104)*, and *clec-35(icb105)* were identified by crossing mutants to the polymorphic CB4856 strain, where 15–25 F2 recombinants selected for loss of *chil-27p::GFP* induction upon extract treatment were pooled in equal proportion to obtain genomic DNA for whole genome sequencing (Novogene, UK). WGS data was analyzed using the CloudMap Hawaiian variant mapping pipeline to identify the causative mutations.[80] Additional alleles were identified by direct WGS of mutants without crossing to CB4856.

Oomycete infection assays

Five *M. humicola* infected animals (filled with spherical sporangia) were added to the lawn of 100 μL *E. coli* OP50 on three 35 mm NGM plates and 20 live L4 animals for each genotype were transferred individually to each plate (n = 60 per condition). Dead animals with visible sporangia were scored every 48 h and live animals were transferred to a new NGM plate with five infected animals to maintain constant pathogen load throughout the experiment. Dead animals without evidence of infection or animals missing from the plate were censored. All infection assays were performed in triplicates at 20°C. Survival curves were plotted using OASIS 2 and statistical significance was evaluated using Log Rank test.

P. aeruginosa PA14 infection assay

P. aeruginosa PA14 were grown overnight in LB broth at 37°C and 100 μL of this culture was spread on 35 mm NGM plates. The plates were allowed to dry for 24 h at RT after which 30 young adults for each strain were moved onto these plates in triplicates (90 worms per condition) followed by incubation at 25°C. Numbers of alive worms were counted every 24 h and were moved onto new PA14 plates every 48 h. Immobile animals and unresponsive to touch were considered as dead. The experiment was performed twice independently. Survival curve was plotted using OASIS 2 and statistical significance was evaluated using Log Rank test.

RNAseq

For transcriptome analysis, animals were first synchronized by bleaching and were treated with *M. humicola* extract for 4 h at L4 stage along with untreated animals as control. After this they were collected for RNA extraction using TRIzol (Invitrogen) and isopropanol/ethanol precipitation. RNA was quantified using NanoDrop (Thermo Scientific) and quality was assessed by gel electrophoresis. The samples were collected from three independent biological repeats for each condition and RNA sequencing was completed by Novogene (UK). Kallisto was used for alignments with the WS283 transcriptome from Wormbase.[76] Count analysis was performed using Sleuth along with a Wald Test to calculate $\log_2$fold changes.[81] All RNAseq data files are publicly available from the NCBI GEO database under the accession number GSE263858.

Microscopy

For performing induction assays with oomycete extracts, day 1 gravid adults were bleached, and the embryos obtained were plated onto standard NGM-OP50 plates at 20°C. Oomycete extracts from *M. humicola*[12] and *H. zoospora*[48] were made as previously described. Extract treatment was performed by adding 150–200 μL of extract on the NGM plate such that it fully covered the OP50 lawn. For most experiments, embryos were treated with extract for 48 h and imaging of L4 stage animals was performed. For specific experiments as described in the results section, extract treatment was performed from L2 or L4 stage onwards and day 1 adults were imaged after 48 h or 24 h respectively. Animals to be imaged were picked into a drop (5μL) of M9 containing sodium azide (25 mM) on an agarose (2%) pad made on a glass slide. To document *chil-27p::GFP* expression, we used a Zeiss Axio Zoom V16 microscope and images were taken using the associated ZEN Microscopy software.

To image *clec-27p::GFP*, animals were mounted on a slide as described above, and were observed at 40x magnification on a Zeiss Compound microscope (AxioScope A1) with images taken using OCULAR (QImaging). To look at transcriptional reporters of *clec-27/35* and *clec-26/36* or co-localization of *clec-35p::mScarlet* and *clec-36p::mScarlet* with neuron-specific markers, confocal microscopy was performed on Leica SP8 inverted confocal microscope at 63x magnification, with excitation of GFP by an Argon 488nm laser and excitation of mScarlet by a He-Ne 594nm laser. To image CEH-37:GFP, L1 stage animals were observed at 100x magnification on Nikon Ti-eclipse epifluorescence microscope with an iKon M DU-934 CCD camera (Andor).

Molecular cloning and transgenesis

For rescue of mutants obtained from the EMS screen, *clec-27* and *clec-35* were PCR amplified from N2 genomic DNA using primers P1 and P2, and P3 and P4 respectively. These were injected in the respective mutants at 20 ng/μL. For rescue of *ceh-37(icb36)*, fosmid (WRM065bE05) carrying the wild-type copy of the gene was injected at 20 ng/μL. To generate clec-27/35 transcriptional reporter strains, a synthetic gene fragment (*clec-35 3′UTR::wrmscarlet::clec-35/27p::GFPo::clec-27 3′UTR*) cloned in pUC57 was obtained from Genewiz. The resulting plasmid, pCV12, was injected in N2 animals at 50 ng/μL. To generate a construct for pan-neuronal expression of *clec-27/35*, a fragment containing *clec-35* was PCR amplified from N2 genomic DNA using primers P5 and P6, a fragment containing *clec-27* was amplified from N2 genomic DNA using primers P7 and P8, a fragment containing T2A was amplified using primers P9 and P10, and all 3 fragments were then inserted into the vector pGO29 (*rab-3p::unc-54 3′UTR*) by Gibson cloning, generating pCV10(*rab-3p::clec-35::T2A::clec-27*). For epidermal rescue, the fragment *clec-35::T2A::clec-27* was PCR amplified from

pCV12 using primers P11 and P12 and was inserted into vector pIR6 (*dpy-7p::unc-54 3′UTR*) by Gibson cloning, generating pCV11(*dpy-7p::clec-35::T2A::clec-27*). For intestinal rescue, the promoter for gene *vha-6* (3kb upstream of TSS) was PCR amplified from N2 genomic DNA using primers P13 and P14 and the vector backbone containing *clec-35::T2A::clec-27* was PCR amplified from pCV12 using primers P15 and P16. The two fragments were assembled by Gibson cloning to make pKL158(*vha-6p::clec-35::T2A::clec-27*). pCV10, pCV11 and pKL158 were injected in *clec-35(icb105)* mutant animals at 5 ng/μL. For neuronal and intestinal expression of *clec-27/35* in *ceh-37(icb36)* mutants, pCV10 and pKL158 were injected in *ceh-37(icb36)* mutant animals at 5 ng/μL. All microinjections included pRJM163 (*bus-1p::GFP*) as the co-injection marker at 25 ng/μL, along with pBJ36 as carrier DNA to bring the total DNA concentration of the mix to 110 ng/μL.

For neuron-specific rescue of *clec-27*, the fragment *clec-27::clec-27 3′UTR* was amplified using the primers P17 and P18, the promoters for neuron-specific expression were amplified using P19 and P20 for *ceh-37p* fragment, P21 and P22 for *odr-10p* fragment, P23 and P24 for *str-1p* fragment, P25 and P26 for *srg-8p* fragment, P27 and P28 for *gcy-33p* fragment, P29 and P30 for the *gcy-15p* fragment. Each neuron-specific promoter fragment was inserted along with the *clec-27::clec-27 3′UTR* fragment into SpeI digested pBJ97 by Gibson cloning, generating the plasmids pKL6(*ceh-37p::clec-27*), pKL7(*odr-10p::clec-27*), pKL4(*str-1p::clec-27*), pKL2(*gcy-15p::clec-27*), pKL3(*gcy-33p::clec-27*), and pKL1(*srg-8p::clec-27*). These plasmids were injected into *clec-27(icb104)* mutant animals at 50 ng/μL, including pRJM163 (*bus-1p::GFP*) as the co-injection marker at 25 ng/μL, along with pBJ36 as carrier DNA to bring the total DNA concentration of the mix to 110 ng/μL.

For AWA specific expression of *clec-35/27*, the *clec-35::T2A::clec-27::unc-54 3′UTR* fragment was PCR amplified from pCV12 using primers P31 and P32. pKL7 was digested with AvrII, generating a backbone containing *odr-7p*, which was assembled by Gibson cloning with the *clec-35::T2A::clec-27::unc-54 3′UTR* fragment, generating pKL8(*odr-7p::clec-35::T2A::clec-27*). For AWB specific expression, the vector backbone containing *clec-35::T2A::clec-27::unc-54 3′UTR* was PCR amplified from pKL8 using primers P33 and P16. The *str-1p* fragment was amplified from pKL4 using primers P34 and P35. The two fragments were then assembled by Gibson cloning, generating pKL128(*str-1p::clec-35::T2A::clec-27*). These plasmids were injected into *ceh-37(icb36)* mutant animals at 50 ng/μL, including pRJM163 (*bus-1p::GFP*) as the co-injection marker at 25 ng/μL, along with pBJ36 as carrier DNA to bring the total DNA concentration of the mix to 110 ng/μL.

For the AWA GFP marker (*odr-10p::GFPo::unc-54*), the *odr-10p* fragment was amplified using primers P36 and P37. The GFPo fragment was amplified using primers P38 and P39. The *unc-54 3′ UTR* fragment was amplified using primers P40 and P41. Linearized vector was amplified using primers P42 and P16 from the pBJ97 plasmid. These three fragments were assembled with the vector by Gibson cloning, generating pKL53. For the AWB GFP marker (*str-1p::GFPo::unc-54 3′UTR*), the *str-1p* fragment was amplified using primers P34 and P43. The GFPo fragment was amplified using primers P38 and P39. The *unc-54 3′ UTR* fragment was amplified using primers P40 and P41. Linearized vector was amplified using primers P42 and P16 from the BJ97 plasmid. These three fragments were assembled with the vector by Gibson cloning, generating pKL54. These plasmids were injected into N2 animals at 40 ng/μL, including PIP1303F (*rpsa-1p::hgb::unc-54 3′UTR*) as the co-injection marker at 15 ng/μL, along with pBJ36 as carrier DNA to bring the total DNA concentration of the mix to 110 ng/μL.

The *clec-26/36* transcriptional reporter was designed with *wrmScarlet* replacing the *clec-36* RNA coding sequence and *gfp* replacing the *clec-26* RNA coding sequence, whilst keeping the *clec-26/36* shared promoter intact. This transcriptional reporter was commercially synthesized (Genewiz) in a pUC-GW-AMP vector. The plasmid was then injected into N2 animals at 50 ng/μL, including pRJM163 (*bus-1p::GFP*) as the co-injection marker at 25 ng/μL, along with pBJ36 as carrier DNA to bring the total DNA concentration of the mix to 110 ng/μL.

For rescue of *clec-26/36* in different tissues, the *vha-6p* (intestinal) promoter fragment was amplified using primers P13 and P44, the *rab-3p* (neuronal) promoter fragment was amplified using primers P45 and P46, the *odr-7p* (AWA) promoter fragment was amplified using primers P47 and P48, and the str-1p (AWB) promoter fragment was amplified using P34 and P49. Each promoter fragment was combined with a linearized vector containing *unc-54 3′ UTR* (amplified using primers P50 and P16 from pKL53), a fragment containing *clec-36::T2A* (amplified from N2 gDNA using primers P51 and P52), and a fragment containing *T2A::clec-26* (amplified from N2 gDNA using primers P53 and P54), generating the plasmids pKL141(*vha-6p::clec-36::T2A::clec-26*), pKL136 (*rab-3p::clec-36::T2A::clec-26*), pKL63(*odr-7p::clec-36::T2A::clec-26*), and pKL130(*str-1p::clec-36::T2A::clec-26*). These plasmids were injected into *clec-26/36 (icb135)* mutant animals at 50 ng/μL, including pRJM163 (*bus-1p::GFP*) as the co-injection marker at 25 ng/μL, along with pBJ36 as carrier DNA to bring the total DNA concentration of the mix to 110 ng/μL.

CRISPR-mediated genome editing

To generate deletions in *clec-26*, *clec-36*, and both simultaneously, two crRNA were used for every deletion with one binding toward the 5′ end of the gene and the other toward the 3′ end. crRNA 1 and 2 used to make *clec-36(icb138)* deletion, crRNA 3 and 4 used to make *clec-26(icb130)* deletion, and crRNA 1 and 4 to delete both the genes *clec-26/36(icb135)* simultaneously. The sequences of all crRNA used can be found in Table S2 as well as the sequence/genomic coordinates of the deleted regions. For the injection mix, 1.4 μL of each crRNA (IDT) (from 34 μM stock) was mixed with 5 μL of tracrRNA (IDT) (from 18 μM stock) and 1 μL of Cas9 protein (IDT) (from 2.5 μg/μL stock) by pipetting several times before incubating at 37°C for 15 min. Following this, pRJM163 (*bus-1p::GFP*) was added at concentration of 25 ng/μL as co-injection marker and nuclease-free water was added to bring up the total volume to 20 μL. The mix was centrifuged at 13000g for 5 min, and a volume of 17 μL was transferred to a new tube, which was then used for injecting the strain MBA281 (*C. elegans* carrying *chil-27p::GFP* reporter). Transgenic F1s were individually picked based on the

presence of *bus-1p::GFP* spot in the tail and genotyping was performed using the following primer pairs: P55 crispr and P56 crispr for *clec-36(icb138)*, P57 crispr and P58 for *clec-26(icb130)*, P59 and P60 for *clec-26/36(icb135).* The sequences of all primers used can be found in Table S2.

RNA interference (RNAi)

RNAi by feeding was used as previously described.[82] The RNAi clone for *ceh-37* and *skn-1* were obtained from the ORFeome Library, while clones for all *clec* genes tested, *old-1*, *vab-3* and *pals-22* were obtained from the Ahringer Library (Source BioScience). For *flor-1* RNAi, a custom-made clone was used.[55] The clones were confirmed by sequencing prior to use. RNAi plates were made by adding 1 mM IPTG (Thermo scientific) to NGM to induce the expression of dsRNA along with 40 μg/mL ampicillin and 10 μg/mL tetracycline to select for the *E. coli* HT115 strain carrying the RNAi clones. For all RNAi treatments (except *skn-1* RNAi), 6 L4 stage animals (P0) were added onto RNAi plates and after 96 h of incubation at 20°C the progeny at late L4/early adult stage was scored. For *skn-1* RNAi, post-embryonic RNAi treatment was performed where embryos collected by bleaching gravid adults were added onto RNAi plates and day 1 adults after 72 h of incubation at 20°C were scored for the phenotype. For experiments involving extract exposure and RNAi treatment, extract was added on the RNAi plates when the progeny was at L2 stage, 48 h prior to scoring at the adult stage. All experiments were performed in biological triplicates, except the RNAi screen in Figure S5A, which was performed once with technical duplicates. At least 50 animals were scored for every condition in each repeat. Statistical significance was evaluated using chi-squared test.

Single molecule fluorescence *in situ* hybridization

smFISH was performed as previously described.[83] Briefly, L2 stage N2 animals were fixed with 4% formaldehyde (Sigma-Aldrich) in 1x PBS (Ambion) for 45 min and were permeabilised with 70% ethanol for 24 h. Hybridization was performed at 30°C for 16 h. Probe sequences can be found in supplementary Table S2. Imaging was performed using the 100x objective in an inverted and fully motorised epifluorescence microscope (Nikon Ti-eclipse) with an iKon M DU-934 CCD camera (Andor) controlled via the NIS-Elements software (Nikon).

Phylogenetic analysis

To identify all the *clec* pairs in the *C. elegans* genome, 1 kb sequence upstream of TSS (predicted promoter region) for all *clec* genes was recovered using WormBase ParaSite followed by BLAST search against *C. elegans* genome. The sequences that aligned with any *clec* gene were identified and 36 *clec* genes present in pairs were identified within the *C. elegans* genome (*clec-128/129*, *clec-131/132*, *clec-62/63*, *clec-158/159*, *clec-167/168*, *clec-197/198*, *clec-73/74*, *clec-83/84*, *clec-45/46*, *clec-34/38*, *clec-29/39*, *clec-23/40*, *clec-26/36*, *clec-27/35*, *clec-22/31*, *clec-24/32*, *clec-245/246*, *clec-255/256*). Among these genes, 4 genes are annotated as pseudogenes (*clec-131*, *clec-159*, *clec-46*, *and clec-23*) on Wormbase and these pairs were eliminated from further analysis. Protein sequences of the remaining 28 paired protein-coding *clec* genes with a total of 992 positions were aligned in MEGA11[78] by MUSCLE and the resulting alignment was used to generate a phylogenetic tree by maximum-likelihood with 500 bootstrap replications under default settings, using a Jones-Taylor-Thornton model with uniform rates among sites, using all sites and Nearest-Neighbour Interchange for the Maximum Likelihood Heuristic Method.

Heterologous *clec* expression and co-immunoprecipitation

Constructs for heterologous expression of various full length CLEC proteins were generated by Gibson assembly of a PCR fragment amplified from *C. elegans* cDNA into EcoRV linearised pKGC3S harboring a C-terminal GFP- or myc-tag (fragments were amplified using the primer pairs P61/P62, P63/P64, P65/P66, P67/P68). *N. benthamiana* plants were grown in a controlled environment growth chamber with a temperature range of 22°C–25°C, humidity of 45–65% and a 16/8-h light/dark cycle. Three-week-old plants were grown in individual pots until infiltration with *Agrobacterium*. *A. tumefaciens* GV3101 was transformed with *clec* constructs and grown overnight in LB with appropriate antibiotics at 28°C. Bacteria were collected and resuspended in infiltration buffer (10 mM MES, 10 mM $MgCl_2$, and 150 μM acetosyringone (pH 5.6) at a final OD_{600} of 0.5 for constructs and 0.05 for p19 in combinations as indicated. Leaf discs were collected 2 dpi and shock frozen until protein extraction. CLEC proteins were extracted by lysis with bead beating (2 min at 1500 rpm). 400 μL extraction buffer (10% (v/v) glycerol, 25 mM Tris, 1 mM EDTA, 150 mM NaCl at pH7.4 with 1 mM PMSF, 1 mM DTT, 0.3% NP-40) was added and tubes incubated on ice for 20 min and regular shaking. The leaf suspension was centrifuged for 10 min at 17,000 xg, the supernatant transferred and centrifuged again for 10 min at 17,000 xg. The supernatant was incubated for 1h at 4°C with equilibrated GFP and Myc beads (Proteintech) successively, and washed 3x with extraction buffer before proteins were eluted with SDS loading buffer at 70°C for 10 min. Samples were run on a NuPAGE 4 to 12%, Bis-Tris Mini gel and then transferred at 30V for 75 min to a nitrocellulose membrane using a Mini gel tank (Invitrogen). Membranes were blocked in 3% BSA in PBST (137 mM NaCl, 12 mM Phosphate, 2.7 mM KCl, pH 7.4, 0.1% tween 20) before adding the primary antibody at 1:1500 dilution (α-GFP, rabbit, Invitrogen; α-myc, rat, Proteintech) for incubation overnight at 4°C. The membrane was washed with PBST before adding the secondary HRP-coupled antibodies at 1:3000 dilution (α-rabbit, sigma) or at 1:3000 dilution (α-rat, Merck). Blots were visualised with ECL (Amersham) on a Licor Odyssey Fc Imaging System.

QUANTIFICATION AND STATISTICAL ANALYSIS

Graphic representation and statistical analysis were performed using the GraphPad Prism 7 software. Data shown in bar graphs indicate mean, and error bars represent standard error of proportion, standard error of the mean, or standard deviation, as indicated in respective figure legends. A chi-squared test, unpaired t test, or Cochran Mantel-Haenszel test was used to evaluate significance as indicated in respective figure legends. Survival data was analyzed using OASIS 2 (https://sbi.postech.ac.kr/oasis2/)[77] and significance was assessed using a log rank test. Results were considered statistically significant when $p < 0.05$. Asterisks in figures indicate corresponding statistical significance as it follows: *$p < 0.05$; **$p < 0.01$; ***$p < 0.001$; ****$p < 0.0001$.